
Test time training enhances in-context learning of nonlinear functions

Kento Kuwataka^{*1,2} Taiji Suzuki^{*1,2}

Abstract

Test-time training (TTT) enhances model performance by explicitly updating designated parameters prior to each prediction to adapt to the test data. While TTT has demonstrated considerable empirical success, its theoretical underpinnings remain limited, particularly for nonlinear models. In this paper, we investigate the combination of TTT with in-context learning (ICL), where the model is given a few examples from the target distribution at inference time. We analyze this framework in the setting of single-index models $y = \sigma_*(\langle \beta, \mathbf{x} \rangle)$, where the feature vector β is drawn from a hidden low-dimensional subspace. For single-layer transformers trained with gradient-based algorithms and adopting TTT, we establish an upper bound on the prediction risk. Our theory reveals that TTT enables the single-layer transformers to adapt to both the feature vector β and the link function σ_* , which vary across tasks. This creates a sharp contrast with ICL alone, which is theoretically difficult to adapt to shifts in the link function. Moreover, we provide the convergence rate with respect to the data length, showing the predictive error can be driven arbitrarily close to the noise level as the context size and the network width grow.

1. Introduction

In-context learning (ICL) is a powerful capability of pre-trained transformers to solve tasks using a few labeled examples provided as input, without updating their weights. This ability has gained increasing attention with the advent of models with massive context windows, as more examples lead to significantly improved performance (Agarwal et al., 2024). This approach has also proven effective for

¹Department of Mathematical Engineering and Information Physics, The University of Tokyo, Tokyo, Japan ²RIKEN AIP, Tokyo, Japan. Correspondence to: Kento Kuwataka <kuwataka-kento954@g.ecc.u-tokyo.ac.jp>, Taiji Suzuki <taiji@mist.i.u-tokyo.ac.jp>.

multimodal tasks (Jiang et al., 2024). From a theoretical perspective, transformers are known to implement algorithms such as linear regression. Recent studies have extended this understanding to nonlinear settings, showing that transformers can learn nonlinear single-index models (Oko et al., 2024) and that softmax attention facilitates data-efficient feature learning (Nishikawa et al., 2025). Nevertheless, ICL faces its inherent limitations: the performance of ICL is fundamentally constrained by factors like the pretraining data (Bigoulaeva et al., 2025) and model architecture (Naim & Asher, 2025).

Test-time training (TTT) has emerged as a promising strategy to overcome these barriers. TTT adapts the model by updating its parameters on the test data before each prediction. This adaptive mechanism has led to strong empirical success across various fields, including large language models (Hu et al., 2025) and video object segmentation (Bertrand et al., 2023). In the context of ICL, TTT can be seamlessly integrated by using the in-context examples as data for task-specific adaptation. For instance, Akyürek et al. (2025) demonstrated that this combination achieves notable improvements on few-shot reasoning benchmarks.

Despite its empirical success, the theoretical foundations of TTT remain underdeveloped. A notable work by Gozeten et al. (2025) established the statistical efficiency of TTT over standard ICL, but their analysis was restricted to linear regression with a linear transformer. This simplified model fails to capture the true potential of TTT’s power on nonlinear, complex tasks. This gap motivates our primary research question:

Does test-time training improve in-context learning in nonlinear settings?

Furthermore, existing theoretical works commonly analyze performance in high-dimensional regimes, showing that the prediction loss is $o_d(1)$ and thus vanishes as the data dimension d grows. In practice, however, this dimension is fixed, making it crucial to understand how the loss behaves as the number of data points n increases. This raises our second key question:

How does the test loss behave when we fix the dimension and increase the data size?

1.1. Our contribution

To address the questions above, we analyze the performance of transformers on learning single-index models, a simple type of nonlinear function. In our setting, each task is defined as

$$\mathbf{x}_1^t, \dots, \mathbf{x}_N^t, \mathbf{x}^t \stackrel{\text{i.i.d.}}{\sim} \mathcal{N}(0, \mathbf{I}_d), y_i^t \approx \sigma_*^t(\langle \beta^t, \mathbf{x}_i^t \rangle) \\ (i = 1, \dots, n)$$

where σ_*^t is an unknown polynomial that varies across tasks, and β^t is drawn from a fixed r -dimensional subspace. Using the in-context data $\mathbf{x}_1, \dots, \mathbf{x}_N$, our model constructs the predictor for the new query \mathbf{x} . We establish a rigorous upper-bound on the predictive risk for a transformer that utilizes TTT. Our main result is as follows:

Theorem 1.1 (Informal). *Consider learning single-index polynomial $\sigma_*^t(\langle \beta^t, \mathbf{x} \rangle)$ with the transformer trained via Algorithm 1. Then, with probability at least 0.99, we can construct the model f_{TF} for each prompt that satisfies $\mathbb{E}[|f_{\text{TF}}(\mathbf{x}^t) - \sigma_*^t(\langle \beta^t, \mathbf{x}^t \rangle)|] = \tilde{O}(m^{-1/2}) + \tilde{O}(\sqrt{\frac{r\sqrt{r}}{N_{\text{test}}}})$, where N_{pt} and T_{pt} are the context length and the number of tasks in pretraining, respectively, N_{test} is the context length in test-time, m is the network width, if $N_{\text{pt}} = T_{\text{pt}} = (d^{\Omega(\text{ie}(\sigma_*^t))} r^2)$ and $N_{\text{test}} = \tilde{\Omega}(r^{\Omega(\text{ge}(\sigma_*^{\text{test}}))})$, where $\text{ie}(\sigma_*)$ and $\text{ge}(\sigma_*)$ are the information exponent and the general exponent of the polynomial σ_* , respectively.*

This theorem ensures the effectiveness of TTT in learning nonlinear single-index models, extending its known applicability to linear models. Our analysis reveals several strengths of our approach:

- **Efficient sample complexity:** Theorem 1.1 implies that $N_{\text{test}} = \tilde{\Omega}(r^{2\vee\Theta(\text{ge}(\sigma_*^{\text{test}}))})$ to ensure low predictive loss $\tilde{O}(\sqrt{\frac{r\sqrt{r}}{N_{\text{test}}}})$, which does not depend on the entire dimension d . This shows that transformers can adapt to the low-dimensionality of β . In addition, this statistical complexity does not depend on either the degree of the polynomial $\text{deg}(\sigma_*^{\text{test}})$ or $\text{ie}(\sigma_*^{\text{test}})$, which outperforms CSQ learners and shows a comparable performance with that of SQ learners.
- **Flexibility for varying nonlinearity:** Our framework allows the link function σ_* to vary across tasks. This adaptability is enabled by TTT, which fine-tunes the MLP layer each time using task-specific test data.
- **Statistical guarantee for practical settings:** We provide an explicit convergence rate with respect to the context length N_{test} . This result offers a statistical guarantee in practical scenarios where the dimensions d, r are large but fixed. This establishes a fundamental advantage over standard ICL: while existing frameworks

(Nishikawa et al., 2025) fail to prove that the predictive risk vanishes as $N_{\text{test}} \rightarrow \infty$, our TTT-based approach ensures that the error can be driven to an arbitrarily small value.

To empirically validate our theoretical predictions, we perform numerical experiments with a 2-layer GPT-2 model in a controlled setting. The results, presented in Figure 1, reveal that while standard ICL struggles to adapt to shifts in the link function σ_* , TTT achieves significantly lower predictive error, which continues to decrease with increasing sequence length. This empirical success validates our theoretical claim: TTT provides the necessary flexibility to achieve exact recovery of task-specific nonlinearities, beyond the architectural limitations of static in-context learning. See section 4 for further details.

1.2. Related works

In-context learning and its theoretical analysis In-context learning (Brown et al., 2020) is transformer’s ability to adapt to the specific task using few labeled examples, without updating any parameters. Agarwal et al. (2024) demonstrated that many in-context examples lead to considerably improved performance, and Jiang et al. (2024) confirmed that many-shot ICL is also beneficial for multimodal tasks. The theoretical background of ICL is extensively studied. For example, a wide array of works (Garg et al., 2023; von Oswald et al., 2023; Zhang et al., 2024b; Gattmiry et al., 2024) have shown that linear transformers can be trained to perform linear regression in-context. As for nonlinear transformers, Cheng et al. (2024) demonstrated that nonlinear transformers learn to perform gradient descent and thus learn nonlinear functions. Also, Nichani et al. (2024) analyzed learning of causal structure by softmax transformer. Recently, Dherin et al. (2025) showed that ICL in a single-transformer block (a self-attention layer and subsequent MLP layer) corresponds to low-rank update in MLP layer. Regarding limitations of ICL, Bigoulaeva et al. (2025) argued that pretraining datasets impose a fundamental limit on the model’s capability with ICL. Furthermore, (Naim & Asher, 2025) demonstrated that the transformer’s ICL ability to generalize functions is limited to certain input values, and found that this limitation comes from layer normalization and softmax attention.

Test-time training Test-time training (Sun et al., 2020; Liu et al., 2021) updates the model using test data before making predictions, thereby addressing distribution shifts. TTT achieved success in many fields. For example, Bertrand et al. (2023) applied TTT for the video object segmentation task and achieved a significant improvement in the performance. Moreover, Hu et al. (2025) analyzed test-time learning of large language models and achieved at least 20%

higher performance on domain knowledge adaptation. Furthermore, Zhang et al. (2025) proposed adopting a large chunk update, and validated the effectiveness of their approach to long-context data through tasks like image sets and language model. As for TTT combined with few-shot prediction, Akyürek et al. (2025) reported that introducing TTT with in-context examples resulted in 6 times higher accuracy in the Abstraction and Reasoning Corpus and a 7.3 percent higher score on BIG-Bench Hard. Finally, regarding the theory behind TTT for in-context learning, Gozeten et al. (2025) analyzed the linear transformer with a single gradient step and characterized the prediction risk of the model with TTT, showing that TTT can mitigate distribution shift.

2. Preliminaries and problem settings

Notations Let $\text{He}_i(z) = (-1)^i e^{\frac{z^2}{2}} \frac{d^i}{dz^i} e^{-\frac{z^2}{2}}$ be the degree- i (probabilist's) Hermite polynomial. \mathbb{S}^{d-1} denotes the unit sphere in \mathbb{R}^d . For matrix \mathbf{A} , we denote its ℓ_2 operator norm and Frobenius norm as $\|\mathbf{A}\|_2$ and $\|\mathbf{A}\|_F$, respectively. For a set S , $\text{Unif}(S)$ denotes the uniform distribution over S . $\tilde{O}, \tilde{\Omega}, \tilde{\Theta}$ means O, Ω, Θ where polylogarithmic terms of d and $1/\varepsilon$ are hidden. O_d, Ω_d, Θ_d means the order with respect to the dimension d, r , while Θ_ε denotes the order in terms of ε .

2.1. In-context learning and test-time training

We consider the basic setting in ICL, which is introduced by Garg et al. (2023) (see Oko et al. (2024) and Lee et al. (2024)). In this setting, the model is given a sequence $(\mathbf{x}_1, y_1, \dots, \mathbf{x}_N, y_N, \mathbf{x})$ called prompt. The labeled pairs $(\mathbf{x}_i, y_i) \in \mathbb{R}^d \times \mathbb{R}$ are called contexts, and $\mathbf{x} \in \mathbb{R}^d$ is referred to as query. The model is asked to predict the output that corresponds to \mathbf{x} based on the context. The context is sometimes abbreviated as $(\mathbf{X}_n, \mathbf{y}_n)$ where $\mathbf{X}_n = (\mathbf{x}_1, \dots, \mathbf{x}_n), \mathbf{y}_n = (y_1, \dots, y_n)$. In this work, we assume that the \mathbf{x} and y are generated as follows:

$$\mathbf{x}_1^t, \dots, \mathbf{x}_N^t, \mathbf{x}^t \stackrel{\text{i.i.d.}}{\sim} \mathcal{N}(0, \mathbf{I}_d), y_i^t = f_*^t(\mathbf{x}_i^t) + \zeta_i, \\ \zeta_i \sim \text{Unif}(-\tau, \tau).$$

ICL aims to predict $y = f_*^t(\mathbf{x}) + \zeta$ by mere observation of the context, without updating parameters for each prompt. However, we introduce test-time training to further enhance the model's accuracy. In pretraining, we train the model with T_{pt} distinct datasets $(\mathbf{x}_1^t, y_1^t, \dots, \mathbf{x}_{N_{pt}}^t, y_{N_{pt}}^t, \mathbf{x}^t, y^t)_{t=1}^{T_{pt}}$, with each prompts consisting of N_{pt} queries. In test-time, we divide the context into four groups with i -th group's length N_i . This means the test-time prompt is $(\mathbf{X}_{N_1}, \mathbf{y}_{N_1}, \mathbf{X}_{N_2}, \mathbf{y}_{N_2}, \mathbf{X}_{N_3}, \mathbf{y}_{N_3}, \mathbf{X}_{N_4}, \mathbf{y}_{N_4}, \mathbf{x})$. Each group of data plays a different role in test-time training: See subsection 2.4 for the detail. Let $N_{test} = \sum_{i=1}^4 N_i$ be the total number of contexts test-time.

For the evaluation of the model $f(\mathbf{x}, \theta)$ with parameter θ , we define prediction risk as

$$\mathcal{R}_f(\theta) = \mathbb{E}[|f(\mathbf{x}, \theta) - y|],$$

where $y = f_*(\mathbf{x}) + \zeta$ and the expectation is taken over the prompt $\mathbf{x}_i, \mathbf{x} \sim \mathcal{D}_{\mathbf{x}}, f_* \sim \mathcal{D}_{f_*}, \zeta_i, \zeta \sim \mathcal{D}_\zeta$. Note that $\mathcal{R}_f(\theta)$ not only depends on the dimensions d, r but also on the context length N .

2.2. Single index model

We consider single-index models for the input-output relationship, where the output depends solely on the direction of the feature vector β . To predict this relationship accurately, the models are expected to learn the target direction β from the high-dimensional data in \mathbb{R}^d . Consequently, single-index models have been extensively studied in machine learning theory (Bai & Lee, 2020; Ba et al., 2022; Bietti et al., 2022; Mousavi-Hosseini et al., 2023; Berthier et al., 2024), particularly to examine adaptability to the low-dimensional subspace. The target function $f_*^t(\mathbf{x})$ is determined as $f_*^t(\mathbf{x}) = \sigma_*^t(\langle \beta^t, \mathbf{x} \rangle)$.

- 1. Feature vector** The feature vector β is chosen uniformly from the unit sphere in an r -dimensional subspace. Let S_r be an r -dimensional linear subspace in \mathbb{R}^d . For each prompt, β^t is uniformly drawn from its support $\text{Supp}(\beta) = \{\beta \mid \beta \in S_r, \|\beta\| = 1\}$.
- 2. Link function** We take $\sigma_*^t(z) = \sum_{i=Q}^P \frac{c_i^t}{i!} \text{He}_i(z)$ where $1 \leq Q \leq P$. We assume P and Q are constants of $O(1)$. The coefficients c_i^t are drawn from any distribution \mathcal{D}_{σ_*} that satisfies

$$\mathbb{E}[c_Q^t] = \Theta(1) \neq 0, \sum_{i=Q}^P (c_i^t)^2 \leq R_c = \Theta(1) \text{ (a.s.)} \\ \text{and } (c_Q^t, \dots, c_P^t) \neq (0, \dots, 0) \text{ (a.s.)}$$

Remark 2.1. We draw a new feature vector β^t and a new link function $\sigma_*^t(z)$ for each prompt. When $r \ll d$, β^t has low-dimensional support. We will later demonstrate that our model can leverage this low-dimensionality. Note that our analysis is also valid when $r = d$. As for the link function, we do not assume a specific distribution of the coefficients c_i : our framework allows different distributions as long as they satisfy the assumptions above.

For simplicity, we assume that $N_{pt}, T_{pt}, N_1, N_2, N_3, N_4 = \text{poly}(d)$, and there exists $\alpha_r > 0$ that $r = \Omega(d^{\alpha_r})$, which means that r grows faster than polylog(d).

The complexity of learning single-index model is governed by three key quantities: the degree of the polynomial $\text{deg}(\sigma_*)$, the information exponent $\text{ie}(\sigma_*)$, and the general exponent $\text{ge}(\sigma_*)$.

- The information exponent (Dudeja & Hsu, 2018; Arous et al., 2021) $\text{ie}(\sigma_*)$ is the smallest non-zero degree of the hermite expansion of σ_* .
- The general exponent (Damian et al., 2024) $\text{ge}(\sigma_*)$ is the minimum of $\text{ie}(f \circ \sigma_*)$ with respect to all the L_2 -measurable transformation f .

By definition, $\text{deg}(\sigma_*) \geq \text{ie}(\sigma_*) \geq \text{ge}(\sigma_*)$ holds. This relationship characterizes the statistical complexity required by different algorithms.

- The kernel method, which relies on pre-determined feature maps, requires the sample complexity $n \gtrsim d^{\Theta(\text{deg}(\sigma_*))}$ to ensure low predictive error (Ghorbani et al., 2020; Donhauser et al., 2021).
- The models with access to correlational statistical query (CSQ), of the form $\mathbb{E}[\phi(\mathbf{x})y]$, require a sample size of $n \gtrsim d^{\Theta(\text{ie}(\sigma_*))}$, known as CSQ lower bound (Damian et al., 2022; Abbe et al., 2023). This improved sample complexity, independent of $\text{deg}(\sigma_*)$, has been achieved by models like two-layer neural network with online SGD (Arous et al., 2021; Damian et al., 2023) or one-step gradient descent (Damian et al., 2022; Dandi et al., 2025).
- For the broader class of statistical queries (SQ), which takes the form $\mathbb{E}[\phi(\mathbf{x}, y)]$, the sample complexity is further improved to $n \gtrsim d^{\Theta(\text{ge}(\sigma_*))}$. This advantage comes from applying nonlinear transformations to the label y , thereby reducing $\text{ie}(\sigma_*)$. Recent works have achieved this complexity by reusing the data (Lee et al., 2024; Arnaboldi et al., 2025) or adjusting the loss function (Joshi et al., 2024). Furthermore, when σ_* is a polynomial, the following result holds:

Lemma 2.2 (Lee et al. (2024), Proposition 6). *It holds*

$$\text{that } \text{ge}(\sigma_*) = \begin{cases} 1 & (\text{if } \sigma_* \text{ is not even}) \\ 2 & (\text{if } \sigma_* \text{ is even}) \end{cases}.$$

Moreover, $\text{ge}(\sigma_) = \min_{j \geq 1} \text{ie}(\sigma_*^j)$ holds.*

This implies that, for any polynomial σ_* , $\text{ge}(\sigma_*) \leq 2$ is a small constant, regardless of $\text{deg}(\sigma_*)$.

Our goal is to achieve the test-time sample complexity of $N_{\text{test}} = r^{\Theta(\text{ge}(\sigma_*))}$, which is independent of the entire dimension d and surpasses the CSQ limit.

2.3. Student model

To facilitate our theoretical analysis, we need to establish a concrete architecture for the student model. We employ a single-layer transformer model, formulated as follows.

In pretraining, we use the same model as Nishikawa et al. (2025). We first construct the embedding \mathbf{E} as

$$\mathbf{E} = \begin{bmatrix} \mathbf{x}_1 & \cdots & \mathbf{x}_N & \mathbf{x} \\ y_1 & \cdots & y_N & 1 \end{bmatrix} \in \mathbb{R}^{(d+1) \times (N+1)}.$$

Then, we apply the softmax attention layer as

$$\begin{aligned} & \text{Attn}(\mathbf{E}) \\ &= \mathbf{W}^V \mathbf{E} \cdot \text{softmax}(\text{Mask}(\rho^{-1} \cdot (\mathbf{W}^K \mathbf{E})^\top \mathbf{W}^Q \mathbf{E})), \end{aligned}$$

where ρ is temperature and $\mathbf{W}^V, \mathbf{W}^K, \mathbf{W}^Q \in \mathbb{R}^{(d+1) \times (d+1)}$ are the parameters for attention layer. The softmax is applied to each column, while the Mask function converts all the elements in the final row into $-\infty$ to prevent the model from focusing on the uninformative final row. We further apply a multi-layer perceptron (MLP) layer. For the activation function, we use ReLU function $\sigma(z) = \max\{0, z\}$ throughout the paper. With the parameters $\mathbf{W}^F \in \mathbb{R}^{m \times (d+1)}$, $\mathbf{b} \in \mathbb{R}^m$, and $\mathbf{a} \in \mathbb{R}^m$ where m is the network width, the model's output is

$$\begin{aligned} f_{\text{IC}}(\Gamma, \mathbf{X}_N, \mathbf{y}_N, \mathbf{x}) &= \text{MLP} \circ \text{Attn}(\mathbf{E})_{:,N+1} \\ &= \mathbf{a}^\top \sigma(\mathbf{W}^F \text{Attn}(\mathbf{E})_{:,N+1} + \mathbf{b}), \end{aligned}$$

where σ is applied entry-wise. Finally, we adopt some simplification. Let $\mathbf{W}^{KQ} = (\mathbf{W}^K)^\top \mathbf{W}^Q \in \mathbb{R}^{(d+1) \times (d+1)}$ and $\mathbf{W}^{FV} = \mathbf{W}^F \mathbf{W}^V \in \mathbb{R}^{(m+1) \times (d+1)}$. We use the following parametrization:

$$\mathbf{W}^{KQ} = \begin{bmatrix} \Gamma & \mathbf{0}_{d \times 1} \\ \mathbf{0}_{1 \times d} & 1 \end{bmatrix}, \quad \mathbf{W}^{FV} = [\mathbf{O}_{(m+1) \times d} \quad \mathbf{v}],$$

for $\Gamma \in \mathbb{R}^{d \times d}$ and $\mathbf{v} \in \mathbb{R}^{(d+1) \times 1}$. This kind of simplification, specifying some of the parameters as zero, is often adopted in many theoretical works on transformers (Zhang et al., 2024a; Huang et al., 2023; Kim & Suzuki, 2025). Overall, the model's output is written as

$$\begin{aligned} & f_{\text{IC}}(\Gamma, \mathbf{X}_N, \mathbf{y}_N, \mathbf{x}) \\ &= \sum_{j=1}^m a_j \sigma \left(v_j \frac{\sum_{i=1}^N y_i e^{y_i / \rho} e^{\mathbf{x}_i^\top \Gamma \mathbf{x} / \rho}}{\sum_{i=1}^N e^{y_i / \rho} e^{\mathbf{x}_i^\top \Gamma \mathbf{x} / \rho}} + b_j \right). \end{aligned}$$

See Appendix A in Nishikawa et al. (2025) for how to derive this equation. At test-time, we adopt low-rank adaptation (LoRA). Specifically, we change the attention matrix Γ^* as $\Gamma_u = \Gamma^* + \mathbf{u}^\top \mathbf{u}$, where Γ^* is fixed during test-time and $\mathbf{u} \in \mathbb{R}^d$ is a trainable parameter vector. Our goal is to find $\hat{\mathbf{u}} \approx \beta$ using test-time context data. See section 2.4 for how test data is used to find $\hat{\mathbf{u}}$. The final prediction of the model is as follows:

$$f_{\text{TF}}(\mathbf{x}, \hat{\mathbf{u}}, \mathbf{v}, \mathbf{a}, \mathbf{b}) = \sum_{j=1}^m a_j \sigma(v_j \langle \hat{\mathbf{u}}, \mathbf{x} \rangle + b_j).$$

Remark 2.3. Incorporating in-context data into the final prediction—a standard practice in existing TTT frameworks (Akyürek et al., 2025)—presents a fundamental trade-off between finite-sample efficiency and asymptotic consistency. In the small-data regime (small N), retaining in-context examples is beneficial, as it compensates for the estimation error of the updated parameters. However, this benefit comes at the cost of an architectural bottleneck in the large-data regime ($N \rightarrow \infty$): the use of the attention mechanism adds unavoidable noise. As Nishikawa et al. (2025) explains, when the context length N is sufficiently large, the denominator of the attention output $N^{-1} \sum_{i=1}^N e^{y_i/\rho} e^{\mathbf{x}_i^\top \Gamma \mathbf{x}/\rho}$ approximates $\mathbb{E}[\exp \sigma_*(\langle \beta, \mathbf{x}_1 \rangle / \rho) \exp(\langle \Gamma_* \mathbf{x}, \mathbf{x}_1 \rangle / \rho)]$. The key of their work is, since $\exp(\langle \Gamma_* \mathbf{x}, \mathbf{x}_1 \rangle / \rho)$ contains all the Hermite coefficients and $\exp \sigma_*(\langle \beta, \mathbf{x}_1 \rangle / \rho)$ has nonzero coefficient for $\text{He}_{\text{ge}(\sigma_*)}$, this attention layer can compute $\langle \beta, \mathbf{x} \rangle^{\text{ge}(\sigma_*)}$. However, this mechanism inevitably retains $\langle \beta, \mathbf{x} \rangle^k$ for degrees $k > \text{ge}(\sigma_*)$, causing an unavoidable prediction error (bias) that persists even as $N \rightarrow \infty$. By contrast, our final predictor omits in-context data and relies solely on the learned parameter $\hat{\mathbf{u}}$, thereby avoiding this asymptotic bias. We adopt this design to demonstrate that TTT can surpass the standard ICL limit and attain exact recovery.

2.4. Training algorithm

We employ a gradient-based training algorithm, as specified in Algorithm 1. The training procedure consists of pretraining and test-time training, with the latter divided into three stages.

- **Pretraining:** We optimize Γ via one-step gradient descent over T_{pt} prompts. This scheme is originally taken from Nishikawa et al. (2025). The effectiveness of one-step gradient descent is confirmed by works such as Ba et al. (2022) and Damian et al. (2022), which demonstrate that one-step gradient already captures the key feature.
- **TTT stage I:** We apply a single gradient descent step to $\mathbf{u}^{(0)}$ with L_2 -regularization. This stage prevents catastrophic forgetting, a phenomenon where the parameter change caused by TTT deprives the model of the fundamental ability to adapt to the original task. The goal of this stage is to find a good initial value of $\mathbf{u}^{(1)}$ that satisfies $\langle \beta, \mathbf{u}^{(1)} \rangle \geq 1/\text{polylog}(d)$. For this stage, we use the output from the attention layer of the original model as a teacher signal, which is defined as $g(\Gamma_*, \mathbf{X}_{N_1}, \mathbf{y}_{N_1}, \mathbf{x}) = \frac{N_1^{-1} \sum_{i=1}^{N_1} y_i e^{y_i/\rho} e^{\mathbf{x}_i^\top \Gamma_* \mathbf{x}}}{N_1^{-1} \sum_{i=1}^{N_1} e^{y_i/\rho} e^{\mathbf{x}_i^\top \Gamma_* \mathbf{x}}}$. In this stage, the query \mathbf{x} do not require ground-truth label y . Therefore, we use N_{new} newly generated vectors $w_1, \dots, w_{N_{new}} \stackrel{\text{i.i.d.}}{\sim} \mathcal{N}(0, \mathbf{I}_d)$ for the query. The ne-

cessity of this stage is further discussed in subsection 3.1.2.

- **TTT stage II:** We continue to optimize \mathbf{u} by applying multi-step online SGD scheme that originates from Lee et al. (2024), using $(\mathbf{X}_{N_2}, \mathbf{y}_{N_2})$ as contexts. In this stage, we use the ground truth $(\mathbf{X}_{N_3}, \mathbf{y}_{N_3})$ as the teacher signal. This stage aims to align \mathbf{u} more closely to the target β . As we will see, increasing the number of the SGD steps leads to the convergence of \mathbf{u} to β .
- **TTT stage III:** Finally, we train the MLP layer to fit to the nonlinear link function σ_*^{test} . Specifically, we randomize \mathbf{v} and \mathbf{b} and optimize \mathbf{a} with ridge regression, following the recipe in Nishikawa et al. (2025). This problem is convex with respect to \mathbf{a} , ensuring that the global optimum can be readily found.

Remark 2.4. While Algorithm 1 involves multiple stages, this structure reflects distinct practical objectives rather than arbitrary complexity. In real-world implementations, pretraining and test-time training naturally operate as separate phases. Furthermore, Stage I utilizes a self-supervised objective for initialization, which fundamentally differs from the supervised objectives in the later stages; thus, it must be treated as a distinct step even in practice. The only structural deviation from a typical implementation is the separation of Stage II (Attention learning) and Stage III (MLP learning). This layer-wise decoupling is primarily introduced for theoretical analysis: it is a standard technique for obtaining rigorous guarantees and has been widely adopted in prior works (Damian et al., 2022; Abbe et al., 2023; Lee et al., 2024; Oko et al., 2024).

3. Main result

Based on the problem settings above, we are now ready to present our main result.

Theorem 1.1 (Formal). *We denote the link function drawn in inference-time as σ_*^{test} . Suppose that $T_{pt}, N_{pt} = \tilde{\Omega}(r^2 d^{Q+2})$, $N_1 = \tilde{\Omega}(r^{\text{ge}(\sigma_*^{\text{test})+2})$, $N_{new} = \tilde{\Omega}(r^{\text{ge}(\sigma_*^{\text{test})+2})$, $N_2 = \tilde{\Theta}(r^2)$. Moreover, we assume that $m, N_{pt}, T_{pt}, N_1, N_2, N_3, N_4 = O(\text{poly}(d))$ and there exists $\alpha_r > 0$ that satisfies $r = \Omega(d^{\alpha_r})$. When we fix d large enough, then there exists $\lambda_{pt}, \lambda_1, \eta_{pt}, \eta_1, \eta_2$ such that the prediction risk is low with probability at least 0.99 over the training data and random initialization. Concretely, for the model trained via Algorithm 1, we have that*

$$\begin{aligned} & |\mathcal{R}_{f_{\text{TF}}}(\mathbf{u}, \mathbf{v}^*, \mathbf{a}^*, \mathbf{b}^*) - \tau| \\ &= \tilde{O}(N_4^{-1/2}) + \tilde{O}(m^{-1/2}) + \tilde{O}\left(\sqrt{\frac{r\sqrt{r}}{N_3}}\right), \end{aligned}$$

with probability at least 0.99.

Algorithm 1 Pretraining and test-time training of transformer

Input: Learning rate $\eta_{pt}, \eta_1, \eta_2$, regularization rate λ_{pt}, λ_1 , initialization scale $\alpha_{pt}, \alpha_1, \alpha_2$, dimensions d, r , temperature ρ .
 $\Gamma(0) \sim \mathbf{I}_d / \sqrt{d}$, $\mathbf{v}(0) \sim \text{Unif}(\{\pm 1\}^m)$, $\mathbf{b}(0) = \mathbf{0}_m$, $\mathbf{a}(0) = \alpha_{pt} \mathbf{1}_m$.
{Pretraining}
 $\Gamma^* \leftarrow \Gamma(0) - \eta_{pt} \frac{1}{2T_{pt}} \sum_{t=1}^{T_{pt}} \nabla_{\Gamma} ((f_{\text{IC}}(\Gamma, \mathbf{X}_{N_{pt}}, \mathbf{y}_{N_{pt}}, \mathbf{x}^t) - y^t)^2 + \lambda_{pt} \|\Gamma\|_F^2)$.
{Test-time Training}
 $\mathbf{a}(0) = \alpha_1 \mathbf{1}_m$.
for $i = 1$ **to** N_1 **do**
 $\mathbf{x}_i \leftarrow \sqrt{r} \Gamma^* \mathbf{x}_i$.
end for
 $\mathbf{u}^{(0)} \sim \mathcal{N}(0, \mathbf{I}_d)$, $\mathbf{u}^{(0)} \leftarrow \sqrt{r} \Gamma^* \mathbf{u}^{(0)}$, $\mathbf{u}^{(0)} \leftarrow \frac{\mathbf{u}^{(0)}}{\sqrt{r} \|\mathbf{u}^{(0)}\|}$.
{Stage I: Weak Recovery}
 Draw $\mathbf{w}_1, \dots, \mathbf{w}_{N_{new}} \stackrel{\text{i.i.d.}}{\sim} \mathcal{N}(0, \mathbf{I}_d)$.
 $b = \frac{1}{N_{new}} \sum_{i=1}^{N_{new}} g(\Gamma^*, \mathbf{X}_{N_1}, \mathbf{y}_{N_1}, \mathbf{w}_i)$,
 $\mathbf{u}^{(1)} = \mathbf{u}^{(0)} - \eta_1 \{ \sqrt{r} \Gamma^* \nabla_{\mathbf{u}} \frac{1}{2N_{new}} \sum_{i=1}^{N_{new}} (f_{\text{IC}}(\Gamma_{\mathbf{u}}, \mathbf{X}_{N_1}, \mathbf{y}_{N_1}, \mathbf{w}_i) - (g(\Gamma^*, \mathbf{X}_{N_1}, \mathbf{y}_{N_1}, \mathbf{w}_i) - b))^2 + \frac{\lambda_1}{2} \nabla_{\mathbf{u}} \|\mathbf{u}\|^2 \}$,
 $\mathbf{u}^{(1)} \leftarrow \frac{\mathbf{u}^{(1)}}{\|\mathbf{u}^{(1)}\|}$.
 $\mathbf{a}(0) = \alpha_2 \mathbf{1}_m$.
for $i = N_1 + 1$ **to** $N_1 + N_2$ **do**
 $\mathbf{x}_i \leftarrow \sqrt{r} \Gamma^* \mathbf{x}_i$.
end for
{Stage II: Strong Recovery}
for $t = 1$ **to** N_3 **do**
 $\mathbf{u}^{(t+1)} = \mathbf{u}^{(t)} - \eta_2 \sqrt{r} \Gamma^* \nabla_{\mathbf{u}} (\frac{1}{2} (f_{\text{IC}}(\Gamma_{\mathbf{u}}, \mathbf{X}_{N_2}, \mathbf{y}_{N_2}, \mathbf{x}_{N_1+N_2+t}) - y_{N_1+N_2+t})^2)$.
 $\mathbf{u}^{(t+1)} \leftarrow \frac{\mathbf{u}^{(t+1)}}{\|\mathbf{u}^{(t+1)}\|}$.
end for
 $b_j^* \sim \text{Unif}([- \log^2 d, \log^2 d])$, $\mathbf{v}^* = \mathbf{v}(0)$.
{Stage III: Training of MLP Layer}
 $\mathbf{a}^* \leftarrow \arg \min_{\mathbf{a}} \frac{1}{2N_4} \sum_{t=N_1+N_2+N_3+1}^{N_1+N_2+N_3+N_4} (f_{\text{TF}}(\mathbf{x}_t, \mathbf{u}^{(N_3+1)}, \mathbf{v}^*, \mathbf{a}, \mathbf{b}^*) - y_t)^2 + \frac{\lambda_2}{2} \|\mathbf{a}\|^2$.
Output: Prediction $f_{\text{TF}}(\mathbf{x}, \mathbf{u}^{(N_3+1)}, \mathbf{v}^*, \mathbf{a}^*, \mathbf{b}^*)$.

The proof is given in Appendix G. Our result has the following advantages compared to previous works.

(i) Nonlinearity While Gozeten et al. (2025) also investigates test-time training combined with ICL, their analysis is restricted to linear datasets and a transformer with linear attention. By contrast, we consider a more complex and general problem of prediction for a single-index model with a nonlinear polynomial. In addition, the student model in our work utilizes nonlinear softmax attention, thereby extending the analysis beyond linear transformers.

(ii) The adaptability to link function Our framework has the flexibility of using a task-specific link function σ_*^t . In the previous work by Nishikawa et al. (2025), the link function is fixed throughout all the tasks (only β varies across different tasks) because the training of the relevant layer is done only in pretraining. In contrast, the use of test-time training allows the model to adapt to the characteristics of each task. Therefore, our algorithm is effective even when the underlying link function varies from one task to another.

(iii) The convergence rate of predictive loss with respect to n The analysis by Nishikawa et al. (2025) guarantees that the ICL risk is $o_d(1)$, but it provides no guarantee that the risk diminishes as $n \rightarrow \infty$. In fact, this is an inherent consequence of adopting softmax attention, as we discussed in Remark 2.3. In contrast, our result overcomes that limitation. When d is a sufficiently large constant, our theory ensures that the prediction risk can be made arbitrarily close to the inevitable noise τ by increasing the context size N_{test} and the network width m . This is because the increase in the test-time context length N_3 allows the vector \mathbf{u} to converge to the ground truth β .

In addition, it is worth noting that we achieve efficient sample complexity. Theorem 1.1 implies that $N_{test} = \tilde{\Omega}(r^{2+\text{ge}(\sigma_*^{\text{test}})})$ to ensure low predictive loss $\tilde{O}(\sqrt{\frac{r\sqrt{r}}{N_{test}}})$, yielding two key benefits. First, our sample complexity does not depend on the entire dimension d , which means this model adapts to the low-dimensionality of β . Second, our sample complexity is independent of either $\text{deg}(\sigma_*^{\text{test}})$ or $\text{ie}(\sigma_*^{\text{test}})$, which breaks the CSQ upper bound. Moreover, for polynomials where $\text{ge}(\sigma_*) \leq 2$ holds, the required number of samples is small. In conclusion, our sample complexity is nearly optimal. It is instructive to compare this with Nishikawa et al. (2025). Although they also achieve sample complexity with these two features ($N_{test} = \tilde{\Omega}(r^{3\text{ge}(\sigma_*)/2})$), their result guarantees convergence with respect to d , not N_{test} . This implies that their result is valid only in the asymptotic limit where $d \rightarrow \infty$. Moreover, they do not provide the convergence rate with respect to d . In contrast, our result holds for any sufficiently large fixed d .

These advantages are further supported by numerical experiments in section 4.

3.1. Proof sketch

The outline of the proof of our main theorem proceeds in three stages. First, we achieve weak recovery—i.e., a non-trivial overlap between β and \mathbf{u} —by leveraging the output of the pretrained attention layer as a teacher signal. The attention mechanism reduces the information exponent of the link function $\text{ie}(\sigma_*)$ to its general exponent $\text{ge}(\sigma_*)$. We exploit this property to significantly accelerate the initial

alignment of \mathbf{u} compared to vanilla SGD. Once weak recovery is established, we show that subsequent training on the ground-truth signal y drives the model toward strong recovery ($\langle \beta, \mathbf{u} \rangle \geq 1 - \varepsilon$). Finally, the optimization of the MLP layer allows the model to adapt to the task-specific nonlinearity of the target link function.

3.1.1. EXPLOITING THE PRETRAINED ATTENTION MATRIX

As shown in Nishikawa et al. (2025), the attention matrix Γ^* after pretraining captures the r -dimensional Span of β :

Lemma 3.1 (Informal, Correspond to Proposition 22 in Nishikawa et al. (2025)). *After running the pretraining in Algorithm 1 with $T_{pt}, N_{pt} = \tilde{\Omega}(r^2 d^{Q+2})$, it holds that*

$$\Gamma^* \approx c_r \mathbb{E}_\beta [\beta \beta^\top]$$

with high probability, where $c_r = \tilde{\Theta}(\sqrt{r})$.

This means that Γ^* can project vectors into the r -dimensional subspace $\text{Supp}(\beta)$. Therefore, by multiplying $\sqrt{r}\Gamma^*$ to the context $\mathbf{X}_{N_1}, \mathbf{X}_{N_2}$ and the gradient (the coefficient \sqrt{r} is just for adjusting the scale), we can make the problem virtually r -dimensional, even though the entire dimension is d . This leads to the sample complexity only scaling up with r , not the whole dimension d .

3.1.2. WEAK RECOVERY

First, we initialize \mathbf{u} by one step gradient descent using the output from the original model $g(\Gamma_*, \mathbf{X}_{N_1}, \mathbf{y}_{N_1}, w_i)$. We do not use the signal y in this process. Intuitively, this self-distillation can be seen as a prevention of catastrophic forgetting. Taking the information from the original model makes the LoRA model similar to the original model, thereby preserving the desired features of the original model.

To clarify why we need to use the original model as teacher, consider training the LoRA model with the true signal y . Then, by calculating the gradient, we can get the following:

Lemma 3.2 (Informal). *The following holds with high probability:*

$$\begin{aligned} & \frac{1}{2} \sqrt{r} \Gamma^* \nabla_{\mathbf{u}} (f_{\text{IC}}(\Gamma, \mathbf{X}_N, \mathbf{y}_N, \mathbf{x}) - y)^2 \\ & \approx \tilde{\Theta}(\alpha m) \langle \beta, \mathbf{u} \rangle \{ (\sqrt{r})^{-(\text{ie}(\sigma_*)-1)} + \langle \beta, \mathbf{u} \rangle^{2(\text{ie}(\sigma_*)-2)} \} \beta. \end{aligned}$$

See Appendix C for details. At initialization $\langle \beta, \mathbf{u} \rangle = \tilde{O}(1/r)$ holds, so the signal strength is $r^{\Theta(\text{ie}(\sigma_*^{\text{test}}))}$. Therefore, when we train \mathbf{u} from the signal y , we need at least $r^{\Theta(\text{ie}(\sigma_*^{\text{test}}))}$ data.

However, using the original model as teacher signal reduces this data length to $r^{\Theta(\text{ge}(\sigma_*^{\text{test}}))}$. As Nishikawa et al. (2025) showed, the attention layer after pretraining can compute $\langle \beta, \mathbf{x} \rangle^{\text{ge}(\sigma_*^{\text{test}})}$ in-context. Then, noting that

$\text{ie}(\text{He}_{\text{ge}(\sigma_*)}) = \text{ge}(\sigma_*)$, when we learn from the original model, the signal strength becomes $r^{\Theta(\text{ge}(\sigma_*^{\text{test}}))}$. This improved signal strength results in the required data length $N_{\text{test}} = r^{\Theta(\text{ge}(\sigma_*^{\text{test}}))}$, which surpasses CSQ limit.

3.1.3. STRONG RECOVERY

Weak recovery is insufficient for reliably predicting $\langle \beta, \mathbf{x} \rangle$ using only \mathbf{u} . Therefore, we further optimize \mathbf{u} until we achieve strong recovery, defined as $\langle \beta, \mathbf{u} \rangle \geq 1 - \varepsilon$ for a small error tolerance $\varepsilon > 0$. The attainment of weak recovery is a crucial turning point; it allows the model to extract a meaningful signal of β from y , significantly reducing the data requirements for the subsequent phase. Specifically, once $\langle \beta, \mathbf{u}^{(1)} \rangle > 1/\text{polylog}(d)$ is established, the signal strength becomes $O(1/\text{polylog}(d))$, which is independent of $\text{ge}(\sigma_*^{\text{test}})$. This independence ensures that the sample size needed for strong recovery remains unaffected by $\text{ge}(\sigma_*^{\text{test}})$. Moreover, our approach achieves superior sample complexity compared to the prior work by Lee et al. (2024). While their work suggested a linear increase in $\langle \beta, \mathbf{u}^{(n)} \rangle$, which resulted in the required data length $N = \Theta_\varepsilon(\varepsilon^{-2})$, we find that beyond a certain point, the error $1 - \langle \beta, \mathbf{u}^{(n)} \rangle$ converges to 0 geometrically. This acceleration yields an improved sample complexity of $N = \Theta_\varepsilon(\frac{1}{\varepsilon} \log \frac{1}{\varepsilon})$. See Appendix E for further details.

3.1.4. ESTIMATION OF THE LINK FUNCTION

Finally, we train MLP layer to predict the link function σ_*^{test} . Following prior work Nishikawa et al. (2025), we show that training MLP layer leads to small empirical loss. Moreover, we derive the upper bound of the predictive risk using Rademacher complexity. See Appendix F for details.

4. Synthetic experiment

We conducted a numerical experiment to examine the effectiveness of TTT compared to ICL. To align the experimental setup with our theoretical framework, we employed a 2-layer GPT-2 model (Radford et al., 2019) to learn Gaussian single-index functions. See Appendix I for further experimental details.

The ambient and intrinsic dimensions were set to $d = r = 4$. For each task t , the data was generated as follows: $\mathbf{x}_1^t, \dots, \mathbf{x}_N^t, \mathbf{x}^t \stackrel{\text{i.i.d.}}{\sim} \mathcal{N}(0, \mathbf{I}_d)$, $\beta^t \sim \text{Unif}(\mathbb{S}^{r-1})$ and $y_i^t = \sigma_*^t(\langle \beta, \mathbf{x}_i \rangle) = \frac{1}{\sqrt{3!}} \text{He}_3(\langle \beta, \mathbf{x}_i \rangle) + \frac{c^t}{\sqrt{4!}} \text{He}_4(\langle \beta, \mathbf{x}_i \rangle)$, where $c^t \sim \text{Unif}(-0.5, 0.5)$. We compared the following two settings:

1. In-context learning, configured as Garg et al. (2023), Oko et al. (2024) and Nishikawa et al. (2025), where the model makes predictions solely based on the

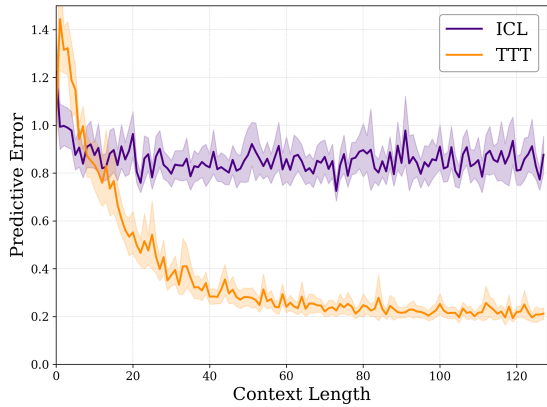


Figure 1. The predictive error of In-context learning (ICL) and Test-time training (TTT) for a pretrained GPT-2 model on single-index polynomials (see Section 4 for details). While vanilla ICL fails to adapt to task-specific link functions, the error for TTT steadily decreases as context length grows. This highlights TTT’s ability to fit the model’s nonlinearity at inference time.

prompt without weight updates. The model was pretrained on a standard task where the link function σ_*^t varied across all prompts.

2. Test-time training: We introduced a strategic pretraining phase: to facilitate the convergence of the attention mechanism on the target subspace, we fixed the link function as $\sigma_*^t = \frac{1}{\sqrt{3!}} \text{He}_3$ during the pretraining. Once pretrained, the model was evaluated on the same challenging task as ICL, where the link function varies and requires test-time adaptation via LoRA.

Figure 1 highlights the result. The predictive error of vanilla ICL remains high and fails to decrease with increasing context length, suggesting that ICL alone cannot adapt to shifts in the link function. In contrast, TTT exhibits steady convergence, with the error diminishing significantly as more context examples are provided. While TTT shows initial instability at very short context lengths due to high-learning-rate updates, it ultimately demonstrates a superior ability to fit task-specific non-linearities. Overall, this result demonstrates a great advantage of TTT: TTT allows the model to adapt to task-specific link functions.

To further assess the capabilities of TTT, we examined its ability to leverage low-dimensional task structures. We fixed the intrinsic dimension at $r = 4$ and compared the predictive error across varying ambient dimensions $d \in \{4, 8, 16\}$. As illustrated in Figure 2, the model performance remains virtually unchanged despite the fourfold increase in the ambient dimension. This empirical result provides strong evidence for our main theorem: the sample complexity of TTT-equipped transformers is governed by the intrinsic dimension r rather than the ambient dimension d , showcasing

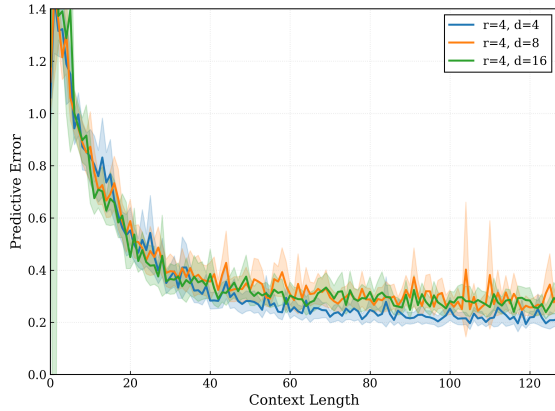


Figure 2. Predictive error of TTT across different ambient dimensions $d \in \{4, 8, 16\}$ with a fixed intrinsic dimension $r = 4$. The overlap of the convergence curves demonstrates that TTT is robust to increases in the ambient dimension, empirically verifying that sample complexity scales with the intrinsic dimensionality r .

the model’s ability to exploit low-dimensional task structures effectively.

5. Conclusion

We have investigated test-time training combined with in-context learning. We provided an upper bound of the predictive loss in terms of m and N . Our result shows that for a large test-time sample size N_{test} , the predictive loss approaches the inevitable noise τ , even when d remains finite.

Future work and limitation We outline some limitations and future research directions.

- We only considered the single-index model where the link function σ_* is a polynomial. Investigating a more general class of input-output relationships is a possible extension of this work.
- In this work, we assumed that the test-time distribution of the feature vector β is the same as in the pretraining. Considering a distribution shift, such as investigating the situation where $\text{Supp}(\beta)_{test}$ is slightly different from $\text{Supp}(\beta)_{pt}$ is another interesting direction.
- Algorithm 1 divides the test-time training into 3 stages, training different layers sequentially. This differs from the typical situation where the entire model is trained at once, as was done in the experiment. Whether a similar upper bound of the predictive risk can be established in such settings remains to be examined.

Impact Statement

This paper presents work whose goal is to advance the field of machine learning. There are many potential societal consequences of our work, none of which we feel must be specifically highlighted here.

Acknowledgement

We thank Yujin Song for his insightful comment and offering us the baseline code for the numerical experiment. KK was partially supported by JST CREST (JPMJCR2015). TS was partially supported by JSPS KAKENHI (24K02905) and JST CREST (JPMJCR2115). This research is supported by the National Research Foundation, Singapore, Infocomm Media Development Authority under its Trust Tech Funding Initiative, and the Ministry of Digital Development and Information under the AI Visiting Professorship Programme (award number AIVP-2024-004). Any opinions, findings and conclusions or recommendations expressed in this material are those of the author(s) and do not reflect the views of National Research Foundation, Singapore, Infocomm Media Development Authority, and the Ministry of Digital Development and Information.

References

- Abbe, E., Adserà, E. B., and Misiakiewicz, T. SGD learning on neural networks: leap complexity and saddle-to-saddle dynamics. In Neu, G. and Rosasco, L. (eds.), *Proceedings of Thirty Sixth Conference on Learning Theory*, volume 195 of *Proceedings of Machine Learning Research*, pp. 2552–2623. PMLR, 12–15 Jul 2023. URL <https://proceedings.mlr.press/v195/abbe23a.html>.
- Agarwal, R., Singh, A., Zhang, L. M., Bohnet, B., Rosias, L., Chan, S. C., Zhang, B., Anand, A., Abbas, Z., Nova, A., Co-Reyes, J. D., Chu, E., Behbahani, F., Faust, A., and Larochelle, H. Many-shot in-context learning. In *The Thirty-eighth Annual Conference on Neural Information Processing Systems*, 2024. URL <https://openreview.net/forum?id=AB6XpMzvqH>.
- Akyürek, E., Damani, M., Zweiger, A., Qiu, L., Guo, H., Pari, J., Kim, Y., and Andreas, J. The surprising effectiveness of test-time training for few-shot learning. In *Forty-second International Conference on Machine Learning*, 2025. URL <https://openreview.net/forum?id=asgBo3FNdg>.
- Arnaboldi, L., Dandi, Y., Krzakala, F., Pesce, L., and Stephan, L. Repetita iuvant: Data repetition allows SGD to learn high-dimensional multi-index functions. *arXiv preprint arXiv:2405.15459*, 2025. URL <https://arxiv.org/abs/2405.15459>.
- Arous, G. B., Gheissari, R., and Jagannath, A. On-line stochastic gradient descent on non-convex losses from high-dimensional inference. *Journal of Machine Learning Research*, 22(106):1–51, 2021. URL <http://jmlr.org/papers/v22/20-1288.html>.
- Ba, J., Erdogdu, M. A., Suzuki, T., Wang, Z., Wu, D., and Yang, G. High-dimensional asymptotics of feature learning: How one gradient step improves the representation. *arXiv preprint arXiv:2205.01445*, 2022. URL <https://arxiv.org/abs/2205.01445>.
- Bai, Y. and Lee, J. D. Beyond linearization: On quadratic and higher-order approximation of wide neural networks. *arXiv preprint arXiv:1910.01619*, 2020. URL <https://arxiv.org/abs/1910.01619>.
- Berthier, R., Montanari, A., and Zhou, K. Learning time-scales in two-layers neural networks. *Foundations of Computational Mathematics*, August 2024. ISSN 1615-3383. doi: 10.1007/s10208-024-09664-9. URL <http://dx.doi.org/10.1007/s10208-024-09664-9>.
- Bertrand, J., Kordopatis-Zilos, G., Kalantidis, Y., and Tolias, G. Test-time training for matching-based video object segmentation. In *Thirty-seventh Conference on Neural Information Processing Systems*, 2023. URL <https://openreview.net/forum?id=9QsdPQlWiE>.
- Bietti, A., Bruna, J., Sanford, C., and Song, M. J. Learning single-index models with shallow neural networks. *arXiv preprint arXiv:2210.15651*, 2022. URL <https://arxiv.org/abs/2210.15651>.
- Bigoulaeva, I., Madabushi, H. T., and Gurevych, I. The inherent limits of pretrained LLMs: The unexpected convergence of instruction tuning and in-context learning capabilities. *arXiv preprint arXiv:2501.08716*, 2025. URL <https://arxiv.org/abs/2501.08716>.
- Brown, T., Mann, B., Ryder, N., Subbiah, M., Kaplan, J. D., Dhariwal, P., Neelakantan, A., Shyam, P., Sastry, G., Askell, A., Agarwal, S., Herbert-Voss, A., Krueger, G., Henighan, T., Child, R., Ramesh, A., Ziegler, D., Wu, J., Winter, C., Hesse, C., Chen, M., Sigler, E., Litwin, M., Gray, S., Chess, B., Clark, J., Berner, C., McCandlish, S., Radford, A., Sutskever, I., and Amodei, D. Language models are few-shot learners. In Larochelle, H., Ranzato, M., Hadsell, R., Balcan, M., and Lin, H. (eds.), *Advances in Neural Information Processing Systems*, volume 33, pp. 1877–1901. Curran Associates, Inc., 2020. URL https://proceedings.neurips.cc/paper_files/paper/2020/file/1457c0d6bfc4967418bfb8ac142f64a-Paper.pdf.

- Cheng, X., Chen, Y., and Sra, S. Transformers implement functional gradient descent to learn non-linear functions in context. *arXiv preprint arXiv:2312.06528*, 2024. URL <https://arxiv.org/abs/2312.06528>.
- Damian, A., Lee, J. D., and Soltanolkotabi, M. Neural networks can learn representations with gradient descent. *arXiv preprint arXiv:2206.15144*, 2022. URL <https://arxiv.org/abs/2206.15144>.
- Damian, A., Nichani, E., Ge, R., and Lee, J. D. Smoothing the landscape boosts the signal for SGD: Optimal sample complexity for learning single index models. In *Thirty-seventh Conference on Neural Information Processing Systems*, 2023. URL <https://openreview.net/forum?id=73XPpmbXH>.
- Damian, A., Pillaud-Vivien, L., Lee, J. D., and Bruna, J. Computational-statistical gaps in Gaussian single-index models. *arXiv preprint arXiv:2403.05529*, 2024. URL <https://arxiv.org/abs/2403.05529>.
- Dandi, Y., Krzakala, F., Loureiro, B., Pesce, L., and Stephan, L. How two-layer neural networks learn, one (giant) step at a time. *arXiv preprint arXiv:2305.18270*, 2025. URL <https://arxiv.org/abs/2305.18270>.
- Dherin, B., Munn, M., Mazzawi, H., Wunder, M., and Gonzalvo, J. Learning without training: The implicit dynamics of in-context learning. *arXiv preprint arXiv:2507.16003*, 2025. URL <https://arxiv.org/abs/2507.16003>.
- Donhauser, K., Wu, M., and Yang, F. How rotational invariance of common kernels prevents generalization in high dimensions. In Meila, M. and Zhang, T. (eds.), *Proceedings of the 38th International Conference on Machine Learning*, volume 139 of *Proceedings of Machine Learning Research*, pp. 2804–2814. PMLR, 18–24 Jul 2021. URL <https://proceedings.mlr.press/v139/donhauser21a.html>.
- Dudeja, R. and Hsu, D. Learning single-index models in Gaussian space. In Bubeck, S., Perchet, V., and Rigollet, P. (eds.), *Proceedings of the 31st Conference On Learning Theory*, volume 75 of *Proceedings of Machine Learning Research*, pp. 1887–1930. PMLR, 06–09 Jul 2018. URL <https://proceedings.mlr.press/v75/dudeja18a.html>.
- Garg, S., Tsipras, D., Liang, P., and Valiant, G. What can transformers learn in-context? a case study of simple function classes. *arXiv preprint arXiv:2208.01066*, 2023. URL <https://arxiv.org/abs/2208.01066>.
- Gatmiry, K., Saunshi, N., Reddi, S. J., Jegelka, S., and Kumar, S. Can looped transformers learn to implement multi-step gradient descent for in-context learning? *arXiv preprint arXiv:2410.08292*, 2024. URL <https://arxiv.org/abs/2410.08292>.
- Ghorbani, B., Mei, S., Misiakiewicz, T., and Montanari, A. Linearized two-layers neural networks in high dimension. *arXiv preprint arXiv:1904.12191*, 2020. URL <https://arxiv.org/abs/1904.12191>.
- Gozeten, H. A., Ildiz, M. E., Zhang, X., Soltanolkotabi, M., Mondelli, M., and Oymak, S. Test-time training provably improves transformers as in-context learners. In *Forty-second International Conference on Machine Learning*, 2025. URL <https://openreview.net/forum?id=bma2FB5MNs>.
- Hu, J., Zhang, Z., Chen, G., Wen, X., Shuai, C., Luo, W., Xiao, B., Li, Y., and Tan, M. Test-time learning for large language models. In *Forty-second International Conference on Machine Learning*, 2025. URL <https://openreview.net/forum?id=iCYbIaGKSR>.
- Huang, Y., Cheng, Y., and Liang, Y. In-context convergence of transformers. *arXiv preprint arXiv:2310.05249*, 2023. URL <https://arxiv.org/abs/2310.05249>.
- Jiang, Y., Irvin, J., Wang, J. H., Chaudhry, M. A., Chen, J. H., and Ng, A. Y. Many-shot in-context learning in multimodal foundation models. *arXiv preprint arXiv:2405.09798*, 2024. URL <https://arxiv.org/abs/2405.09798>.
- Joshi, N., Misiakiewicz, T., and Srebro, N. On the complexity of learning sparse functions with statistical and gradient queries. *arXiv preprint arXiv:2407.05622*, 2024. URL <https://arxiv.org/abs/2407.05622>.
- Kim, J. and Suzuki, T. Transformers provably solve parity efficiently with chain of thought. In *The Thirteenth International Conference on Learning Representations*, 2025. URL <https://openreview.net/forum?id=n2NidsYDop>.
- Kingma, D. P. and Ba, J. Adam: A method for stochastic optimization. *arXiv preprint arXiv:1412.6980*, 2017. URL <https://arxiv.org/abs/1412.6980>.
- Lee, J. D., Oko, K., Suzuki, T., and Wu, D. Neural network learns low-dimensional polynomials with SGD near the information-theoretic limit. *arXiv preprint arXiv:2406.01581*, 2024. URL <https://arxiv.org/abs/2406.01581>.
- Liu, Y., Kothari, P., van Delft, B., Bellot-Gurlet, B., Mordan, T., and Alahi, A. Ttt++: When does self-supervised test-time training fail or thrive? In *Neural*

- Information Processing Systems*, 2021. URL <https://api.semanticscholar.org/CorpusID:247410579>.
- Mousavi-Hosseini, A., Park, S., Girotti, M., Mitliagkas, I., and Erdogdu, M. A. Neural networks efficiently learn low-dimensional representations with SGD. In *The Eleventh International Conference on Learning Representations*, 2023. URL <https://openreview.net/forum?id=6taykzqcPD>.
- Naim, O. and Asher, N. Analyzing limits for in-context learning. *arXiv preprint arXiv:2502.03503*, 2025. URL <https://arxiv.org/abs/2502.03503>.
- Nichani, E., Damian, A., and Lee, J. D. How transformers learn causal structure with gradient descent. *arXiv preprint arXiv:2402.14735*, 2024. URL <https://arxiv.org/abs/2402.14735>.
- Nishikawa, N., Song, Y., Oko, K., Wu, D., and Suzuki, T. Nonlinear transformers can perform inference-time feature learning. In *Forty-second International Conference on Machine Learning*, 2025. URL <https://openreview.net/forum?id=xQTSvP57C3>.
- Oko, K., Song, Y., Suzuki, T., and Wu, D. Pretrained transformer efficiently learns low-dimensional target functions in-context. In *The Thirty-eighth Annual Conference on Neural Information Processing Systems*, 2024. URL <https://openreview.net/forum?id=uHcG5Y6fdB>.
- Radford, A., Wu, J., Child, R., Luan, D., Amodei, D., and Sutskever, I. Language models are unsupervised multitask learners. 2019. URL <https://api.semanticscholar.org/CorpusID:160025533>.
- Sun, Y., Wang, X., Liu, Z., Miller, J., Efros, A. A., and Hardt, M. Test-time training with self-supervision for generalization under distribution shifts. *arXiv preprint arXiv:1909.13231*, 2020. URL <https://arxiv.org/abs/1909.13231>.
- von Oswald, J., Niklasson, E., Randazzo, E., Sacramento, J., Mordvintsev, A., Zhmoginov, A., and Vladymyrov, M. Transformers learn in-context by gradient descent. *arXiv preprint arXiv:2212.07677*, 2023. URL <https://arxiv.org/abs/2212.07677>.
- Zhang, R., Frei, S., and Bartlett, P. L. Trained transformers learn linear models in-context. *Journal of Machine Learning Research*, 25(49):1–55, 2024a. URL <http://jmlr.org/papers/v25/23-1042.html>.
- Zhang, R., Wu, J., and Bartlett, P. L. In-context learning of a linear transformer block: Benefits of the MLP component and one-step GD initialization. *arXiv preprint arXiv:2402.14951*, 2024b. URL <https://arxiv.org/abs/2402.14951>.
- Zhang, T., Bi, S., Hong, Y., Zhang, K., Luan, F., Yang, S., Sunkavalli, K., Freeman, W. T., and Tan, H. Test-time training done right. *arXiv preprint arXiv:2505.23884*, 2025. URL <https://arxiv.org/abs/2505.23884>.

Contents

1	Introduction	1
1.1	Our contribution	2
1.2	Related works	2
2	Preliminaries and problem settings	3
2.1	In-context learning and test-time training	3
2.2	Single index model	3
2.3	Student model	4
2.4	Training algorithm	5
3	Main result	5
3.1	Proof sketch	6
3.1.1	Exploiting the pretrained attention matrix	7
3.1.2	Weak recovery	7
3.1.3	Strong recovery	7
3.1.4	Estimation of the link function	7
4	Synthetic experiment	7
5	Conclusion	8
A	Definition of high probability events	13
B	Pretraining	13
C	Gradient calculation	14
D	One step gradient descent for weak recovery	20
E	Strong recovery	22
F	Training MLP layer	28
G	Proof of the Theorem 1.1	30
H	Additional Lemmas	31
H.1	Pretrained matrix	31
I	Experimental details	34

A. Definition of high probability events

Definition A.1. We say that an event A occurs with high probability when the following holds:

$$1 - P(A) \leq O(d^{-C_*}),$$

where C_* is a sufficiently large constant that is independent of d and r .

Note that we can redefine C_* to be sufficiently large if needed. A basic example is the Gaussian tail bound. When $x \sim \mathcal{N}(0, 1)$ and $t > 0$, we have

$$P(|x| > t) \leq 2 \exp(-t^2/2).$$

Thus, by letting $t = \sqrt{2C_* \log d}$, we see that

$$P(|x| > \sqrt{2C_* \log d}) \leq 2d \exp(-C_*) = O(d^{-C_*}).$$

In such a situation, we say that $|x| = O(\sqrt{\log d})$ with high probability.

When A_1, \dots, A_M occurs with high probability where $M = \text{poly}(d)$, then the intersection $A_1 \cap A_2 \cap \dots \cap A_M$ occurs with high probability. In this paper, we assume that $N_{pt}, T_{pt}, N_1, N_2, N_3, N_4, m = O(\text{poly}(d))$. Because of this assumption, when we take the intersection of high probability events A_1, \dots, A_M , $M = \text{poly}(d)$ is satisfied.

B. Pretraining

We follow the pretraining algorithm that was considered in Nishikawa et al. (2025). In the original paper, the link function σ_* is fixed across all tasks, whereas in this paper, the link function varies depending on the tasks. We should take this difference into account and ensure that the pretraining algorithm works properly even in our setting.

Lemma 3.1 (Formal). *After running the pretraining in Algorithm 1 with $T_{pt}, N_{pt} = \tilde{\Omega}(r^2 d^{Q+2})$, it holds that*

$$\Gamma^* = \frac{1}{r^{1/2} \log^{C_\kappa} d} (r \mathbb{E}_\beta[\beta \beta^\top] + \mathbf{N})$$

with high probability over the data distribution, where $\|\mathbf{N}\|_F = O_d(1/\sqrt{d})$ holds, where C_κ can be taken to be sufficiently large.

Proof. We only consider the difference between our settings and Nishikawa et al. (2025). See Section C of Nishikawa et al. (2025) for the original argument.

If we fix t , we may apply Lemma 19 and Lemma 20 in Nishikawa et al. (2025). In addition to that, since the norm upper bound remains unchanged, we can bound the difference between the expectation and the actual value just like Eq.(C.3) and Eq.(C.4) in Lemma 21 of Nishikawa et al. (2025). What remains is to calculate $\mathbb{E}_{\mathbf{x}, \beta, t}[yz^k \beta \mathbf{x}^\top] = (\rho\sqrt{d})^{-k} \mathbb{E}_\beta[\mathbb{E}_{\mathbf{x}, t}[\sigma_*^t(\langle \beta, \mathbf{x} \rangle) (\langle \beta, \mathbf{x} \rangle)^k] \beta \beta^\top] + (\rho\sqrt{d})^{-k} k \mathbb{E}_\beta[\mathbb{E}_{\mathbf{x}, t}[\sigma_*^t(\langle \beta, \mathbf{x} \rangle) (\langle \beta, \mathbf{x} \rangle)^{k-1}] \beta \beta^\top]$. Because of the definition of $\text{ie}(\sigma_*)$, $\mathbb{E}_{\mathbf{x}, \beta, t}[yz^k \beta \mathbf{x}^\top] = 0$ when $k < Q - 1$. As we assume that $\mathbb{E}_t[c_Q] = \Theta(1)$, when $k = Q - 1$, we see that

$$\begin{aligned} \mathbb{E}_\beta[\mathbb{E}_{\mathbf{x}, t}[\sigma_*^t(\langle \beta, \mathbf{x} \rangle) (\langle \beta, \mathbf{x} \rangle)^k] \beta \beta^\top] &\asymp \mathbb{E}_\beta[\mathbb{E}_{\mathbf{x}}[\mathbb{E}_t[c_Q] \text{He}_{Q-1}(\langle \beta, \mathbf{x} \rangle) \langle \beta, \mathbf{x} \rangle^{Q-1}] \beta \beta^\top] \\ &\asymp (\rho\sqrt{d})^{-(Q-1)} \mathbb{E}_\beta[\beta \beta^\top], \end{aligned}$$

and this is the main term that is proportional to $\mathbb{E}_\beta[\beta \beta^\top]$. This means that we can use the same argument as Nishikawa et al. (2025) with $\text{ie}(\sigma_*) = Q$. \square

Let $\kappa = \log^{-C_\kappa} d$. In other words, κ satisfies $\kappa = \Theta(\log^{-C_\kappa} d)$ where C_κ can be taken sufficiently large.

Lemma B.1. *Suppose that the context length satisfies $N_1 = \tilde{\Omega}(r^{\text{ge}(\sigma_*)+1})$. Then, it holds with high probability that*

$$g(\Gamma^*, \mathbf{X}_{N_1}, \mathbf{y}_{N_1}, \mathbf{x}) = P'_1 + P'_2 \left(\frac{\langle \mathbf{x}, \beta \rangle}{\sqrt{r}} \right)^{\text{ge}(\sigma_*)} + n_3,$$

where $P'_1 = o_d(1)$, $P'_2 = \Theta_d((\log d)^{-C_{P_2}})$ and $n_3 = o_d(P'_2 r^{-\text{ge}(\sigma_*)/2-1/2} \log^{-2 \text{deg}(\sigma_*)+2} d)$.

Proof. When $N_1 = \tilde{\Omega}(r^{\text{ge}(\sigma_*)+1})$, the (h.o.t.) in the proof of Proposition 11 in Nishikawa et al. (2025) can be evaluated as $o(\rho^{-1}P_2r^{-\text{ge}(\sigma_*)/2-1/2}\log^{-2\text{deg}(\sigma_*)+2}d)$ by carefully examining the term. Using this fact, the same argument as the proof of Proposition 11 in Nishikawa et al. (2025) yields the result. \square

C. Gradient calculation

For the sake of simplicity, we write σ_*^{test} as σ_* , and $f_{\text{IC}}(\Gamma, \mathbf{X}_N, \mathbf{y}_N, \mathbf{x}) = \sum_{j=1}^m a_j \sigma \left(v_j \frac{\sum_{i=1}^{N_1} y_i e^{y_i/\rho} e^{\mathbf{x}_i^* \top \Gamma_u \mathbf{x} / \rho}}{\sum_{i=1}^{N_1} e^{y_i/\rho} e^{\mathbf{x}_i^* \top \Gamma_u \mathbf{x} / \rho}} + b_j \right)$ as $f_{\text{IC}}(\mathbf{x})$. Let $\Gamma_u = \Gamma^* + uu^\top$, $\mathbf{x}_i^* = \sqrt{r}\Gamma^* \mathbf{x}_i$, $\beta^* = \sqrt{r}\Gamma^* \beta$. We define L_m as $|\{j \in \{1, 2, \dots, m\} \mid v_j(0) = 1\}|$. Moreover, let us define A_i, B_i as $\bar{\sigma}_*(z) \exp((\bar{\sigma}_*(z)) = \sum_{i \geq 0} \frac{A_i}{i!} z^i$, and $\exp((\bar{\sigma}_*(z)) = \sum_{i \geq 0} \frac{B_i}{i!} z^i$, where

$$\bar{\sigma}_*(z) := \begin{cases} \frac{\sigma_*(z)}{\rho} & \left(\text{if } \left| \frac{\sigma_*(z)}{\rho} \right| \leq \frac{1}{\log d} \right) \\ 0 & \text{(otherwise)} \end{cases}.$$

Lemma C.1. Take $\rho = \Theta((\log d)^{C_\rho})$ where C_ρ is a constant sufficiently large. Let α be the initial scale of the MLP parameters a_j . Suppose that \mathbf{u} satisfies $\|\mathbf{u}\| = C_u \leq 1$ and $\langle \mathbf{u}, \mathbf{x}_i^* \rangle = C_u \tilde{O}_d(1)$. Then

$$\sqrt{r}\Gamma^* \frac{\partial f_{\text{IC}}}{\partial \mathbf{u}} = \alpha L_m \left\{ \sqrt{r}\Gamma^* \mathbf{x} \cdot (\gamma(\mathbf{x}, y) \langle \beta^*, \mathbf{u} \rangle + \sqrt{r}\Gamma^* \gamma(\mathbf{x}, y) \langle \mathbf{x}, \mathbf{u} \rangle \beta^* + \sqrt{r}\Gamma^* \mathbf{x} \cdot \mathbf{n}_1 + \langle \mathbf{x}, \mathbf{u} \rangle \mathbf{n}_2) \right\},$$

where

$$\gamma(\mathbf{x}, y) = P_0 + P_1 z + \dots + P_{\text{ie}(\sigma)-1} z^{\text{ie}(\sigma)-1} + \dots$$

is satisfied with $z = \langle \beta, \sqrt{r}\Gamma^{*\top} \Gamma_u \mathbf{x} \rangle / \rho$, and $\mathbf{n}_1 = \tilde{O} \left(C_u \sqrt{\frac{1}{N_1}} \right)$ and $\mathbf{n}_2 = \tilde{O} \left(\sqrt{\frac{r}{N_1}} \right)$ hold.

Note that from Lemma H.5, the condition $\langle \mathbf{u}, \mathbf{x}_i^* \rangle = C_u \tilde{O}_d(1)$ is satisfied at the initialization.

Proof. Let

$$\begin{aligned} \pi_1(\mathbf{x}, y) &= \frac{1}{N_1} \sum_{i=1}^{N_1} \frac{y_i}{\rho} e^{y_i/\rho} e^{\mathbf{x}_i^* \top \Gamma_u \mathbf{x} / \rho}, \\ \pi_2(\mathbf{x}, y) &= \frac{1}{N_1} \sum_{i=1}^{N_1} e^{y_i/\rho} e^{\mathbf{x}_i^* \top \Gamma_u \mathbf{x} / \rho}, \\ \xi_1(\mathbf{x}, y) &= \frac{1}{N_1} \sum_{i=1}^{N_1} \frac{y_i}{\rho} e^{y_i/\rho} e^{\mathbf{x}_i^* \top \Gamma_u \mathbf{x} / \rho} \{ \langle \mathbf{x}_i^*, \mathbf{u} \rangle \mathbf{x} + \langle \mathbf{u}, \mathbf{x} \rangle \mathbf{x}_i^* \}, \\ \xi_2(\mathbf{x}, y) &= \frac{1}{N_1} \sum_{i=1}^{N_1} e^{y_i/\rho} e^{\mathbf{x}_i^* \top \Gamma_u \mathbf{x} / \rho} \{ \langle \mathbf{x}_i^*, \mathbf{u} \rangle \mathbf{x} + \langle \mathbf{u}, \mathbf{x} \rangle \mathbf{x}_i^* \}. \end{aligned}$$

Then, we can write the gradient of f_{IC} with respect to \mathbf{u} as

$$\frac{\partial f_{\text{IC}}}{\partial \mathbf{u}} = \sum_{j=1}^m a_j \sigma' \left(v_j \frac{\sum_{i=1}^{N_1} y_i e^{y_i/\rho} e^{\mathbf{x}_i^* \top \Gamma_u \mathbf{x} / \rho}}{\sum_{i=1}^{N_1} e^{y_i/\rho} e^{\mathbf{x}_i^* \top \Gamma_u \mathbf{x} / \rho}} + b_j \right) \cdot \frac{\xi_1 \pi_2 - \xi_2 \pi_1}{\pi_2^2}.$$

First, from the assumption $\langle \mathbf{u}, \mathbf{x}_i^* \rangle = C_u \tilde{O}_d(1)$ with $C_u \leq 1$ and Lemma H.1, we can see that

$$\mathbf{x}_i^* uu^\top \mathbf{x} = \langle \mathbf{x}_i^*, \mathbf{u} \rangle \langle \mathbf{u}, \mathbf{x} \rangle = \tilde{O}_d(1).$$

Therefore, by taking C_ρ sufficiently large, we can say $\mathbf{x}_i^* \top \Gamma_u \mathbf{x} / \rho = o_d(1)$ with high probability. Hence, following the same argument as Proposition 11 in Nishikawa et al. (2025), we can say that the content of $\rho'(\cdot)$ is $P_1(1 + o(1))$ using the positive constant P_1 . Therefore, $\rho'(\cdot) = 1$ if and only $v_j = 1$, which means that

$$\frac{\partial f_{\text{IC}}}{\partial \mathbf{u}} = \alpha L_m \frac{\xi_1 \pi_2 - \xi_2 \pi_1}{\pi_2^2}.$$

Next, we evaluate the term $\frac{\xi_1 \pi_2 - \xi_2 \pi_1}{\pi_2^2}$. For that purpose, we first derive the expectation of each component of this term, and then bound the deviation of its actual value from the expectation. Let $k_\rho = \frac{1}{2}(\exp(\tau/\rho) + \exp(-\tau/\rho))$, then the following holds:

$$\mathbb{E}_{\mathbf{x}_1, \zeta_1} [e^{\bar{\sigma}_*(\langle \beta, \mathbf{x}_1 \rangle)/\rho + \zeta_1/\rho} e^{\mathbf{x}_1^{*\top} \Gamma_u \mathbf{x}/\rho} \mathbf{x}_1^*] = k_\rho \mathbb{E}_{\mathbf{x}_1} [e^{\sigma_*(\langle \beta, \mathbf{x}_1 \rangle)} e^{\mathbf{x}_1^{*\top} \Gamma_u \mathbf{x}/\rho} \mathbf{x}_1^*] \quad (1)$$

$$= k_\rho \mathbb{E}_{\mathbf{x}_1} \left[\sum_{i \geq 0} \frac{B_i}{i!} \text{He}_i(\langle \beta, \mathbf{x}_1 \rangle) e^{\mathbf{x}_1^{*\top} \Gamma_u \mathbf{x}/\rho} \mathbf{x}_1^* \right] \quad (2)$$

$$= \sqrt{r} \Gamma^* k_\rho \beta \mathbb{E}_{\mathbf{x}_1} \left[\sum_{i \geq 0} \frac{B_{i+1}}{i!} \text{He}_i(\langle \beta, \mathbf{x}_1 \rangle) e^{\mathbf{x}_1^{*\top} \Gamma_u \mathbf{x}/\rho} \right] \quad (3)$$

$$+ \sqrt{r} \Gamma^* k_\rho \frac{\Gamma_u \mathbf{x}}{\rho} \mathbb{E}_{\mathbf{x}_1} \left[\sum_{i \geq 0} \frac{B_i}{i!} \text{He}_i(\langle \beta, \mathbf{x}_1 \rangle) e^{\mathbf{x}_1^{*\top} \Gamma_u \mathbf{x}/\rho} \right], \quad (4)$$

(recall that $z = \langle \beta, \sqrt{r} \Gamma^{*\top} \Gamma_u \mathbf{x} \rangle / \rho$). Here, we used Stein's lemma to derive the final equality. The expectation in the second term of the RHS can be calculated as

$$\begin{aligned} & \mathbb{E}_{\mathbf{x}_1} \left[\sum_{i \geq 0} \frac{B_i}{i!} \text{He}_i(\langle \beta, \mathbf{x}_1 \rangle) e^{\mathbf{x}_1^{*\top} \Gamma_u \mathbf{x}/\rho} \right] \\ &= \mathbb{E}_{\mathbf{x}_1} \left[\sum_{i \geq 0} \frac{B_i}{i!} \text{He}_i(\langle \beta, \mathbf{x}_1 \rangle) \sum_{j \geq 0} \frac{1}{j!} \left(\frac{\|\sqrt{r} \Gamma^{*\top} \Gamma_u \mathbf{x}\|}{\rho} \right)^j \exp\left(-\frac{\|\sqrt{r} \Gamma^{*\top} \Gamma_u \mathbf{x}\|^2}{2\rho^2}\right) \text{He}_j\left(\left\langle \mathbf{x}_1, \frac{\sqrt{r} \Gamma^{*\top} \Gamma_u \mathbf{x}}{\|\sqrt{r} \Gamma^{*\top} \Gamma_u \mathbf{x}\|} \right\rangle\right) \right] \\ &= \sum_{i \geq 0} \frac{B_i}{i!} \left(\frac{\|\sqrt{r} \Gamma^{*\top} \Gamma_u \mathbf{x}\|}{\rho} \right)^i \exp\left(-\frac{\|\sqrt{r} \Gamma^{*\top} \Gamma_u \mathbf{x}\|^2}{2\rho^2}\right) \left\langle \beta, \frac{\sqrt{r} \Gamma^{*\top} \Gamma_u \mathbf{x}}{\|\sqrt{r} \Gamma^{*\top} \Gamma_u \mathbf{x}\|} \right\rangle^i \\ &= \exp\left(-\frac{\|\sqrt{r} \Gamma^{*\top} \Gamma_u \mathbf{x}\|^2}{2\rho^2}\right) \left(\sum_{i \geq 0} \frac{B_i}{i!} \langle \beta, \sqrt{r} \Gamma^{*\top} \Gamma_u \mathbf{x}/\rho \rangle^i \right). \end{aligned}$$

The expectation in the first term of Eq. (4) can be evaluated in a similar way, and we obtain:

$$\begin{aligned} & \mathbb{E}_{\mathbf{x}_1, \zeta_1} [e^{\bar{\sigma}_*(\langle \mathbf{x}_1, \beta \rangle)/\rho + \zeta_1/\rho} e^{\mathbf{x}_1^{*\top} \Gamma_u \mathbf{x}/\rho} \mathbf{x}_1^*] \\ &= \sqrt{r} \Gamma^* k_\rho \beta \exp\left(-\frac{\|\sqrt{r} \Gamma^{*\top} \Gamma_u \mathbf{x}\|^2}{2\rho^2}\right) \left(\sum_{i \geq 0} \frac{B_{i+1}}{i!} z^i \right) \\ & \quad + \sqrt{r} \Gamma^* \frac{k_\rho}{\rho} \Gamma_u \mathbf{x} \exp\left(-\frac{\|\sqrt{r} \Gamma^{*\top} \Gamma_u \mathbf{x}\|^2}{2\rho^2}\right) \left(\sum_{i \geq 0} \frac{B_i}{i!} z^i \right). \end{aligned} \quad (5)$$

Similarly, using $k'_\rho := \frac{\tau}{2\rho}(\exp(\tau/\rho) - \exp(-\tau/\rho))$, we have that

$$\begin{aligned} & \mathbb{E}_{\mathbf{x}_1, \zeta_1} \left[\frac{\bar{\sigma}_*(\langle \mathbf{x}_1, \beta \rangle) + \zeta_1}{\rho} e^{\bar{\sigma}_*(\langle \mathbf{x}_1, \beta \rangle)/\rho + \zeta_1/\rho} e^{\mathbf{x}_1^{*\top} \Gamma_u \mathbf{x}/\rho} \mathbf{x}_1^* \right] \\ &= \sqrt{r} \Gamma^* k_\rho \exp\left(-\frac{\|\sqrt{r} \Gamma^{*\top} \Gamma_u \mathbf{x}\|^2}{2\rho^2}\right) \left(\sum_{i \geq 0} \frac{A_{i+1}}{i!} z^i \right) \beta + \sqrt{r} \Gamma^* \frac{k_\rho}{\rho} \exp\left(-\frac{\|\sqrt{r} \Gamma^{*\top} \Gamma_u \mathbf{x}\|^2}{2\rho^2}\right) \left(\sum_{i \geq 0} \frac{A_i}{i!} z^i \right) \Gamma_u \mathbf{x} \\ & \quad + \sqrt{r} \Gamma^* k'_\rho \exp\left(-\frac{\|\sqrt{r} \Gamma^{*\top} \Gamma_u \mathbf{x}\|^2}{2\rho^2}\right) \left(\sum_{i \geq 0} \frac{B_{i+1}}{i!} z^i \right) \beta + \sqrt{r} \Gamma^* \frac{k'_\rho}{\rho} \exp\left(-\frac{\|\sqrt{r} \Gamma^{*\top} \Gamma_u \mathbf{x}\|^2}{2\rho^2}\right) \left(\sum_{i \geq 0} \frac{B_i}{i!} z^i \right) \Gamma_u \mathbf{x}. \end{aligned}$$

Let $F_1 = \frac{1}{N_1} \sum_{i=1}^{N_1} \left[\frac{y_i}{\rho} e^{y_i/\rho} e^{\mathbf{x}_i^* \top \Gamma_u \mathbf{x}/\rho} \mathbf{x}_i^* \right]$ and $F_2 = \frac{1}{N_1} \sum_{i=1}^{N_1} [e^{y_i/\rho} e^{\mathbf{x}_i^* \top \Gamma_u \mathbf{x}/\rho} \mathbf{x}_i^*]$. Then, the expectation of ξ_1 and ξ_2 can be written as $\mathbb{E}_{\mathbf{x}_1, \zeta_1} [\xi_1] = \langle \mathbb{E}[F_1], \mathbf{u} \rangle \mathbf{x} + \langle \mathbf{u}, \mathbf{x} \rangle \mathbb{E}[F_1]$ and $\mathbb{E}_{\mathbf{x}_1, \zeta_1} [\xi_2] = \langle \mathbb{E}[F_2], \mathbf{u} \rangle \mathbf{x} + \langle \mathbf{u}, \mathbf{x} \rangle \mathbb{E}[F_2]$ respectively.

Based on the argument above, the term $\frac{\xi_1 \pi_2 - \xi_2 \pi_1}{\pi_2^2}$ is concentrated on

$$(\mathbb{E}[\pi_2])^{-2} \{ \langle \mathbb{E}[F_1] \mathbb{E}[\pi_2], \mathbf{u} \rangle \mathbf{x} + \langle \mathbf{u}, \mathbf{x} \rangle \mathbb{E}[F_1] \mathbb{E}[\pi_2] - \langle \mathbb{E}[F_2] \mathbb{E}[\pi_1], \mathbf{u} \rangle \mathbf{x} - \langle \mathbf{u}, \mathbf{x} \rangle \mathbb{E}[F_2] \mathbb{E}[\pi_1] \}.$$

Also, following the same argument to obtain Eq. (5), we have

$$\mathbb{E}_{\mathbf{x}_1, \zeta_1} \left[e^{\bar{\sigma}_*(\langle \mathbf{x}_1, \beta \rangle) / \rho + \zeta_1 / \rho} e^{\mathbf{x}_1^* \top \Gamma_u \mathbf{x} / \rho} \right] = k_\rho \exp \left(\frac{\|\sqrt{r} \Gamma^* \Gamma_u \mathbf{x}\|^2}{2\rho^2} \right) \left(\sum_{i \geq 0} \frac{B_i}{i!} z^i \right),$$

and

$$\begin{aligned} & \mathbb{E}_{\mathbf{x}_1, \zeta_1} \left[\frac{\bar{\sigma}_*(\langle \mathbf{x}_1, \beta \rangle) + \zeta_1}{\rho} e^{\bar{\sigma}_*(\langle \mathbf{x}_1, \beta \rangle) / \rho + \zeta_1 / \rho} e^{\mathbf{x}_1^* \top \Gamma_u \mathbf{x} / \rho} \right] \\ &= k_\rho \exp \left(\frac{\|\sqrt{r} \Gamma^* \Gamma_u \mathbf{x}\|^2}{2\rho^2} \right) \left(\sum_{i \geq 0} \frac{A_i}{i!} z^i \right) + k'_\rho \exp \left(\frac{\|\sqrt{r} \Gamma^* \Gamma_u \mathbf{x}\|^2}{2\rho^2} \right) \left(\sum_{i \geq 0} \frac{B_i}{i!} z^i \right). \end{aligned}$$

Using these result, we obtain that

$$\begin{aligned} & (\mathbb{E}_{\mathbf{x}_1, \zeta_1} [\pi_2])^{-2} (\mathbb{E}_{\mathbf{x}_1, \zeta_1} [F_1] \mathbb{E}_{\mathbf{x}_1, \zeta_1} [\pi_2] - \mathbb{E}_{\mathbf{x}_1, \zeta_1} [F_2] \mathbb{E}_{\mathbf{x}_1, \zeta_1} [\pi_1]) \\ &= \sqrt{r} \Gamma^* \left(k_\rho \sum_{i \geq 0} \frac{B_i}{i!} z^i \right)^{-2} \times \\ & \left\{ \left[k_\rho \left(\sum_{i \geq 0} \frac{A_{i+1}}{i!} z^i \right) \beta + \frac{k_\rho}{\rho} \left(\sum_{i \geq 0} \frac{A_i}{i!} z^i \right) \Gamma_u \mathbf{x} + k'_\rho \left(\sum_{i \geq 0} \frac{B_{i+1}}{i!} z^i \right) \beta + \frac{k'_\rho}{\rho} \left(\sum_{i \geq 0} \frac{B_i}{i!} z^i \right) \Gamma_u \mathbf{x} \right] \cdot k_\rho \left(\sum_{i \geq 0} \frac{B_i}{i!} z^i \right) \right. \\ & \left. - \left[k_\rho \beta \left(\sum_{i \geq 0} \frac{B_{i+1}}{i!} z^i \right) + \frac{k_\rho}{\rho} \Gamma_u \mathbf{x} \left(\sum_{i \geq 0} \frac{B_i}{i!} z^i \right) \right] \cdot \left[k_\rho \left(\sum_{i \geq 0} \frac{A_i}{i!} z^i \right) + k'_\rho \left(\sum_{i \geq 0} \frac{B_i}{i!} z^i \right) \right] \right\} \\ &= \sqrt{r} \Gamma^* \left(k_\rho \sum_{i \geq 0} \frac{B_i}{i!} z^i \right)^{-2} \left\{ \left[k_\rho \left(\sum_{i \geq 0} \frac{A_{i+1}}{i!} z^i \right) \beta + k'_\rho \left(\sum_{i \geq 0} \frac{B_{i+1}}{i!} z^i \right) \beta \right] \cdot k_\rho \left(\sum_{i \geq 0} \frac{B_i}{i!} z^i \right) \right. \\ & \left. - k_\rho \beta \left(\sum_{i \geq 0} \frac{B_{i+1}}{i!} z^i \right) \cdot \left[k_\rho \left(\sum_{i \geq 0} \frac{A_i}{i!} z^i \right) + k'_\rho \left(\sum_{i \geq 0} \frac{B_i}{i!} z^i \right) \right] \right\}. \end{aligned}$$

Therefore, we can expand this value using z . Specifically,

$$(\mathbb{E}_{\mathbf{x}_1, \zeta_1} [\pi_2])^{-2} (\mathbb{E}_{\mathbf{x}_1, \zeta_1} [F_1] \mathbb{E}_{\mathbf{x}_1, \zeta_1} [\pi_2] - \mathbb{E}_{\mathbf{x}_1, \zeta_1} [F_2] \mathbb{E}_{\mathbf{x}_1, \zeta_1} [\pi_1]) = \sqrt{r} \Gamma^* (P_0 + P_1 z + \dots) \beta$$

holds. By letting $\gamma(\mathbf{x}, y) = P_0 + P_1 z + \dots$, we obtain

$$\frac{\mathbb{E}[\xi_1] \mathbb{E}[\pi_2] - \mathbb{E}[\xi_2] \mathbb{E}[\pi_1]}{\mathbb{E}[\pi_2]^2} = \mathbf{x} \cdot (\gamma(\mathbf{x}, y) \langle \sqrt{r} \Gamma^* \beta, \mathbf{u} \rangle) + \gamma(\mathbf{x}, y) \langle \mathbf{x}, \mathbf{u} \rangle \sqrt{r} \Gamma^* \beta.$$

Following the same argument as Lemma 20 in Nishikawa et al. (2025) yields the order of P_i .

Next we deal with the deviation from the expectation. Using the same technique as Lemma 18 in Nishikawa et al. (2025), we have

$$\frac{1}{N_1} \sum_{i=1}^{N_1} \frac{y_i}{\rho} e^{y_i/\rho} e^{\mathbf{x}_i^* \top \Gamma_u \mathbf{x} / \rho} = \mathbb{E}_{\mathbf{x}_1, \zeta_1} \left[\frac{\bar{\sigma}_*(\langle \mathbf{x}_1, \beta \rangle) + \zeta_1}{\rho} e^{\bar{\sigma}_*(\langle \mathbf{x}_1, \beta \rangle) / \rho + \zeta_1 / \rho} e^{\mathbf{x}_1^* \top \Gamma_u \mathbf{x} / \rho} \right] + \tilde{O}(N_1^{-1/2}),$$

and

$$\frac{1}{N_1} \sum_{i=1}^{N_1} e^{y_i/\rho} e^{\mathbf{x}_i^* \top \Gamma_u \mathbf{x}/\rho} = \mathbb{E}_{\mathbf{x}_1, \zeta_1} \left[e^{\bar{\sigma}_*(\langle \mathbf{x}_1, \beta \rangle)/\rho + \zeta_1/\rho} e^{\mathbf{x}_1^* \top \Gamma_u \mathbf{x}/\rho} \right] + \tilde{O}(N_1^{-1/2}).$$

Moreover, noting that $\sqrt{r}\Gamma^* \mathbf{x}_i^* = \tilde{O}(\sqrt{r})$ (see Lemma H.4), from Lemma H.6, we have

$$\begin{aligned} & \frac{1}{N_1} \sum_{i=1}^{N_1} \sqrt{r}\Gamma^* \frac{y_i}{\rho} e^{y_i/\rho} e^{\mathbf{x}_i^* \top \Gamma_u \mathbf{x}/\rho} \mathbf{x}_i^* \\ &= \sqrt{r}\Gamma^* \mathbb{E}_{\mathbf{x}_1, \zeta_1} \left[\frac{\bar{\sigma}_*(\langle \mathbf{x}_1, \beta \rangle) + \zeta_1}{\rho} e^{\bar{\sigma}_*(\langle \mathbf{x}_1, \beta \rangle)/\rho + \zeta_1/\rho} e^{\mathbf{x}_1^* \top \Gamma_u \mathbf{x}/\rho} \mathbf{x}_1^* \right] + \tilde{O}(r^{1/2} N_1^{-1/2}), \end{aligned}$$

and

$$\frac{1}{N_1} \sum_{i=1}^{N_1} \sqrt{r}\Gamma^* e^{y_i/\rho} e^{\mathbf{x}_i^* \top \Gamma_u \mathbf{x}/\rho} \mathbf{x}_i^* = \sqrt{r}\Gamma^* \mathbb{E}_{\mathbf{x}_1, \zeta_1} \left[e^{\bar{\sigma}_*(\langle \mathbf{x}_1, \beta \rangle)/\rho + \zeta_1/\rho} e^{\mathbf{x}_1^* \top \Gamma_u \mathbf{x}/\rho} \mathbf{x}_1^* \right] + \tilde{O}(r^{1/2} N_1^{-1/2}).$$

Hence, we obtain that

$$\sqrt{r}\Gamma^* \pi_2^{-2} (F_1 \pi_2 - F_2 \pi_1) = \frac{\text{poly}(z)\beta + \delta_2}{\text{poly}(z) + \delta_1},$$

for some δ_1 and δ_2 which satisfy $\delta_1 = \tilde{O}(1/\sqrt{N_1})$ and $\delta_2 = \tilde{O}\left(\sqrt{\frac{r}{N_1}}\right)$ with high probability. Let $\mathbf{n}_2 = \sqrt{r}\Gamma^* \{\pi_2^{-2} (F_1 \pi_2 - F_2 \pi_1) - \gamma(\mathbf{x}, y)\beta\}$, then $\mathbf{n}_2 = \tilde{O}\left(\sqrt{\frac{r}{N_1}}\right)$ holds.

Also, noting that $\langle \mathbf{x}_i^*, \mathbf{u} \rangle = C_u \tilde{O}_d(1)$ with high probability, it holds that

$$\begin{aligned} & \frac{1}{N_1} \sum_{i=1}^{N_1} \frac{y_i}{\rho} e^{y_i/\rho} e^{\mathbf{x}_i^* \top \Gamma_u \mathbf{x}/\rho} \langle \mathbf{x}_i^*, \mathbf{u} \rangle \\ &= \mathbb{E}_{\mathbf{x}_1, \zeta_1} \left[\frac{\bar{\sigma}_*(\langle \mathbf{x}_1, \beta \rangle) + \zeta_1}{\rho} e^{\bar{\sigma}_*(\langle \mathbf{x}_1, \beta \rangle)/\rho + \zeta_1/\rho} e^{\mathbf{x}_1^* \top \Gamma_u \mathbf{x}/\rho} \langle \mathbf{x}_1^*, \mathbf{u} \rangle \right] + \tilde{O}(C_u N_1^{-1/2}), \end{aligned}$$

and

$$\frac{1}{N_1} \sum_{i=1}^{N_1} e^{y_i/\rho} e^{\mathbf{x}_i^* \top \Gamma_u \mathbf{x}/\rho} \langle \mathbf{x}_i^*, \mathbf{u} \rangle = \mathbb{E}_{\mathbf{x}_1, \zeta_1} \left[e^{\bar{\sigma}_*(\langle \mathbf{x}_1, \beta \rangle)/\rho + \zeta_1/\rho} e^{\mathbf{x}_1^* \top \Gamma_u \mathbf{x}/\rho} \langle \mathbf{x}_1^*, \mathbf{u} \rangle \right] + \tilde{O}(C_u N_1^{-1/2}).$$

Therefore, letting $n_1 = \pi_2^{-2} \{ \langle F_1, \mathbf{u} \rangle \pi_2 - \langle F_2, \mathbf{u} \rangle \pi_1 \} - \gamma(\mathbf{x}, y) \langle \beta^*, \mathbf{u} \rangle$, we obtain that $n_1 = \tilde{O}(C_u \sqrt{\frac{1}{N_1}})$.

In summary, we obtain that

$$\sqrt{r}\Gamma^* \frac{\xi_1 \pi_2 - \xi_2 \pi_1}{\pi_2^2} = \sqrt{r}\Gamma^* [\mathbf{x} \cdot (\gamma(\mathbf{x}, y) \langle \beta^*, \mathbf{u} \rangle) + \gamma(\mathbf{x}, y) \langle \mathbf{x}, \mathbf{u} \rangle \beta^*] + \sqrt{r}\Gamma^* \mathbf{x} \cdot n_1 + \langle \mathbf{x}, \mathbf{u} \rangle \mathbf{n}_2,$$

where $n_1 = \tilde{O}\left(C_u \sqrt{\frac{1}{N_1}}\right)$ and $\mathbf{n}_2 = \tilde{O}\left(\sqrt{\frac{r}{N_1}}\right)$. □

Lemma C.2. *The norm of the vector $\|\sqrt{r}\Gamma^* \frac{\partial f_{\text{IC}}}{\partial \mathbf{u}}\|$ has sub-Weibull tail with tail index $1/(P+2)$.*

Proof. It suffices to show that $\left\| \sqrt{r}\Gamma^* \frac{\xi_1 \pi_2 - \xi_2 \pi_1}{\pi_2^2} \right\|$ has sub-Weibull tail. Note that $\frac{\xi_1 \pi_2 - \xi_2 \pi_1}{\pi_2^2} = \frac{\xi_1}{\pi_2} - \frac{\xi_2}{\pi_2} \frac{\pi_1}{\pi_2}$. Therefore we examine $\frac{\xi_1}{\pi_2}$, $\frac{\xi_2}{\pi_2}$ and $\frac{\pi_1}{\pi_2}$. Let us define

$$p_i = \frac{e^{\mathbf{x}_i^* \top \Gamma_u \mathbf{x}/\rho}}{\sum_{i=1}^{N_1} e^{y_i/\rho} e^{\mathbf{x}_i^* \top \Gamma_u \mathbf{x}/\rho}},$$

then the following holds:

$$\frac{\xi_1}{\pi_2} = \sum_{i=1}^{N_1} p_i \frac{y_i}{\rho} \{ \langle \mathbf{x}_i^*, \mathbf{u} \rangle \mathbf{x} + \langle \mathbf{u}, \mathbf{x} \rangle \mathbf{x}_i^* \}$$

$$\begin{aligned}\frac{\xi_2}{\pi_2} &= \sum_{i=1}^{N_1} p_i \{ \langle \mathbf{x}_i^*, \mathbf{u} \rangle \mathbf{x} + \langle \mathbf{u}, \mathbf{x} \rangle \mathbf{x}_i^* \} \\ \frac{\pi_1}{\pi_2} &= \sum_{i=1}^{N_1} p_i \frac{y_i}{\rho}\end{aligned}$$

By the triangle inequality, we have

$$\left\| \frac{\xi_1}{\pi_2} \right\| \leq \sum_{i=1}^{N_1} p_i \frac{y_i}{\rho} \| \langle \mathbf{x}_i^*, \mathbf{u} \rangle \mathbf{x} + \langle \mathbf{u}, \mathbf{x} \rangle \mathbf{x}_i^* \|.$$

By further applying the Cauchy-Schwarz inequality, we have

$$\left\| \frac{\xi_1}{\pi_2} \right\| \leq \left(\sum_{i=1}^{N_1} p_i^2 \right) \left(\sum_{i=1}^{N_1} \frac{y_i^2}{\rho^2} \| \langle \mathbf{x}_i^*, \mathbf{u} \rangle \mathbf{x} + \langle \mathbf{u}, \mathbf{x} \rangle \mathbf{x}_i^* \|^2 \right).$$

Note that $\sum_{i=1}^{N_1} p_i^2 \leq 1$. Next, we can see that

$$y_i^2 \| \langle \mathbf{x}_i^*, \mathbf{u} \rangle \mathbf{x} + \langle \mathbf{u}, \mathbf{x} \rangle \mathbf{x}_i^* \|^2 \leq 2y_i^2 \| \langle \mathbf{x}_i^*, \mathbf{u} \rangle \mathbf{x} \|^2 + 2y_i^2 \| \langle \mathbf{u}, \mathbf{x} \rangle \mathbf{x}_i^* \|^2$$

Since $y_i = \sigma_*(\langle \beta, \mathbf{x} \rangle) + \zeta_i$, the tail probability of each term is almost equal to that of $\text{poly}(t)$ where $t \sim \mathcal{N}(0, 1)$, which means $y_i^2 \| \langle \mathbf{x}_i^*, \mathbf{u} \rangle \mathbf{x} \|^2$ and $y_i^2 \| \langle \mathbf{u}, \mathbf{x} \rangle \mathbf{x}_i^* \|^2$ have sub-Weibull tail with tail index $2/(2P+4)$. This means that $\left\| \frac{\xi_1}{\pi_2} \right\|$ has sub-Weibull tail with tail index $1/(P+2)$. By applying the same argument, you can see that $\frac{\xi_2}{\pi_2} \frac{\pi_1}{\pi_2}$ has sub-Weibull tail. Therefore, considering that $\| \sqrt{r} \Gamma^* \|_2$ is a finite constant, $\| \sqrt{r} \Gamma^* \frac{\partial f_{\text{IC}}}{\partial \mathbf{u}} \|$ has sub-Weibull tail with tail index $1/(P+2)$. \square

Lemma 3.2 (formal). *It holds that*

$$\begin{aligned}& \frac{1}{2} \sqrt{r} \Gamma^* \nabla_{\mathbf{u}} (f_{\text{IC}}(\mathbf{x}) - y)^2 \\ &= \Theta(\alpha m) \langle \beta, \mathbf{u} \rangle \frac{\beta}{\kappa^{\text{ie}(\sigma_*)+1} \rho^{\text{ie}(\sigma_*)}} \{ (\kappa \sqrt{r})^{-(\text{ie}(\sigma_*)-1)} (1 + O(1/\sqrt{d})) + \langle \beta, \mathbf{u} \rangle^{2\text{ie}(\sigma_*)-2} (1 + O(1/\sqrt{d})) \} \\ & \quad + \tilde{O}(\alpha^2 m^2 C_u \sqrt{r}) + \tilde{O} \left(\alpha m C_u \sqrt{\frac{r}{N_1}} \right) + \nu,\end{aligned}$$

with high probability, where ν satisfies $\nu = \tilde{O}(\alpha m C_u \sqrt{r})$ with high probability and $\mathbb{E}_{\mathbf{x}}[\nu] = 0$. Moreover, $\|\nu\|$ has sub-Weibull tail.

Proof. Note that

$$\frac{1}{2} \sqrt{r} \Gamma^* \nabla_{\mathbf{u}} (f_{\text{IC}}(\mathbf{x}) - y)^2 = f_{\text{IC}}(\mathbf{x}) \cdot \sqrt{r} \Gamma^* \nabla_{\mathbf{u}} f_{\text{IC}}(\mathbf{x}) - y \cdot \sqrt{r} \Gamma^* \nabla_{\mathbf{u}} f_{\text{IC}}(\mathbf{x}). \quad (6)$$

First, we analyze the first term of the RHS. Since $y_i = \tilde{O}_p(1)$, we have that

$$|f_{\text{IC}}(\mathbf{x})| \leq \alpha m \left| \frac{\sum_{i=1}^{N_1} y_i e^{y_i/\rho} e^{\mathbf{x}_i^* \Gamma_u \mathbf{x} / \rho}}{\sum_{i=1}^{N_1} e^{y_i/\rho} e^{\mathbf{x}_i^* \Gamma_u \mathbf{x} / \rho}} \right| = \tilde{O}_p(\alpha m).$$

Moreover, from Lemma C.1, it holds that

$$\sqrt{r} \Gamma^* \frac{\partial f_{\text{IC}}}{\partial \mathbf{u}} = \alpha L_m \{ \sqrt{r} \Gamma^* \mathbf{x} \cdot (\gamma(\mathbf{x}, y) \langle \beta^*, \mathbf{u} \rangle + \sqrt{r} \Gamma^* \gamma(\mathbf{x}, y) \langle \mathbf{x}, \mathbf{u} \rangle \beta^* + \sqrt{r} \Gamma^* \mathbf{x} \cdot \mathbf{n}_1 + \langle \mathbf{x}, \mathbf{u} \rangle \mathbf{n}_2) \},$$

where $\sqrt{r} \Gamma^* \mathbf{x} = \tilde{O}(\sqrt{r})$ (See Lemma H.4) and $\gamma(\mathbf{x}, y) = \tilde{O}(1)$ with high probability, which means that $\sqrt{r} \Gamma^* \frac{\partial f_{\text{IC}}}{\partial \mathbf{u}} = \tilde{O}_p(\alpha m C_u \sqrt{r})$. Therefore, we obtain

$$f_{\text{IC}}(\mathbf{x}) \cdot \sqrt{r} \Gamma^* \nabla_{\mathbf{u}} f_{\text{IC}}(\mathbf{x}) = \tilde{O}_p(\alpha^2 m^2 C_u \sqrt{r}).$$

Next, we evaluate the second term of Eq. (6). For that purpose, let

$$\nu = y \cdot \sqrt{r}\Gamma^* \nabla_{\mathbf{u}} f_{\text{IC}}(\mathbf{x}) - \mathbb{E}_{\mathbf{x}}[y \cdot \sqrt{r}\Gamma^* \nabla_{\mathbf{u}} f_{\text{IC}}(\mathbf{x})].$$

By noticing that $y = \tilde{O}_p(1)$ and $\sqrt{r}\Gamma^* \nabla_{\mathbf{u}} f_{\text{IC}}(\mathbf{x}) = \tilde{O}(\alpha m C_u \sqrt{r})$ with high probability, we have

$$\nu = \tilde{O}_p(\alpha m C_u \sqrt{r}).$$

Moreover, $\mathbb{E}_{\mathbf{x}}[\nu] = 0$ by definition, and $\|\nu\|$ has sub-Weibull tail from Lemma C.2. Thus, what remains is to calculate $\mathbb{E}_{\mathbf{x}}[y \cdot \sqrt{r}\Gamma^* \nabla_{\mathbf{u}} f_{\text{IC}}(\mathbf{x})]$:

$$\begin{aligned} & \mathbb{E}_{\mathbf{x}}[y \alpha L_m \{ \sqrt{r}\Gamma^* \mathbf{x} \cdot \gamma(\mathbf{x}, y) \langle \beta^*, \mathbf{u} \rangle + \sqrt{r}\Gamma^* \gamma(\mathbf{x}, y) \langle \mathbf{x}, \mathbf{u} \rangle \beta^* \}] \\ &= \alpha L_m \langle \beta^*, \mathbf{u} \rangle \mathbb{E}_{\mathbf{x}}[\sqrt{r}\Gamma^* \mathbf{x} \sigma_*(\langle \beta, \mathbf{x} \rangle)(P_0 + P_1 z + \dots)] \\ & \quad + \alpha L_m \sqrt{r}\Gamma^* \beta^* \mathbb{E}_{\mathbf{x}}[\langle \mathbf{u}, \mathbf{x} \cdot \sigma_*(\langle \beta, \mathbf{x} \rangle)(P_0 + P_1 z + \dots) \rangle]. \end{aligned} \quad (7)$$

Now, we calculate $\mathbb{E}_{\mathbf{x}}[\sqrt{r}\Gamma^* \mathbf{x} \sigma_*(\langle \beta, \mathbf{x} \rangle) z^k]$ in order to investigate $\mathbb{E}_{\mathbf{x}}[\sqrt{r}\Gamma^* \mathbf{x} \sigma_*(\langle \beta, \mathbf{x} \rangle)(P_0 + P_1 z + \dots)]$:

$$\begin{aligned} & \mathbb{E}_{\mathbf{x}}[\sqrt{r}\Gamma^* \mathbf{x} \sigma_*(\langle \beta, \mathbf{x} \rangle) z^k] \\ &= \sqrt{r}\Gamma^* \{ \mathbb{E}_{\mathbf{x}}[\sigma'_*(\langle \beta, \mathbf{x} \rangle) z^k] \beta + \mathbb{E}_{\mathbf{x}}[\sigma_*(\langle \beta, \mathbf{x} \rangle) k z^{k-1}] \Gamma_u^\top \beta \} \end{aligned} \quad (8)$$

holds from Stein's lemma, and when $k < \text{ie}(\sigma_*) - 1$, $\mathbb{E}_{\mathbf{x}}[\sigma'_*(\langle \beta, \mathbf{x} \rangle) z^k] = 0$ from the definition of the information exponent. When $k = \text{ie}(\sigma_*) - 1$, we have that

$$\sqrt{r}\Gamma^* \mathbb{E}_{\mathbf{x}}[\sigma'_*(\langle \beta, \mathbf{x} \rangle) z^k] \asymp \sqrt{r}\Gamma^* \beta \left(\frac{\langle \beta, \sqrt{r}\Gamma_u^\top \Gamma^* \beta \rangle}{\rho} \right)^{\text{ie}(\sigma_*) - 1},$$

and from Lemma H.7, it holds that

$$\beta^* = \sqrt{r}\Gamma^* \beta = \kappa^{-1}(\beta + O(1/\sqrt{d})),$$

and

$$\begin{aligned} \langle \beta, \sqrt{r}\Gamma_u^\top \Gamma^* \beta \rangle &= \langle \Gamma_u \beta, \sqrt{r}\Gamma^* \beta \rangle \\ &= \langle \Gamma^* \beta, \sqrt{r}\Gamma^* \beta \rangle + \langle \beta, \mathbf{u} \rangle \langle \mathbf{u}, \sqrt{r}\Gamma^* \beta \rangle \\ &= (\sqrt{r}\kappa^2)^{-1}(1 + O(1/\sqrt{d})) + \kappa^{-1} \langle \beta, \mathbf{u} \rangle \{ \langle \beta, \mathbf{u} \rangle + O(1/\sqrt{d}) \} \\ &= (\sqrt{r}\kappa^2)^{-1}(1 + O(1/\sqrt{d})) + \kappa^{-1} \langle \beta, \mathbf{u} \rangle^2 \{ 1 + O(1/\sqrt{d}) \} \end{aligned}$$

with high probability. By ignoring small terms, this yields that

$$\begin{aligned} & \sqrt{r}\Gamma^* \beta \left(\frac{\langle \beta, \sqrt{r}\Gamma_u^\top \Gamma^* \beta \rangle}{\rho} \right)^{\text{ie}(\sigma_*) - 1} \\ &= \frac{P_{\text{ie}(\sigma_*) - 1} \beta}{\kappa^{\text{ie}(\sigma_*)} \rho^{\text{ie}(\sigma_*) - 1}} \{ (\kappa\sqrt{r})^{-(\text{ie}(\sigma_*) - 1)} (1 + O(1/\sqrt{d})) + \langle \beta, \mathbf{u} \rangle^{2\text{ie}(\sigma_*) - 2} (1 + O(1/\sqrt{d})) \}. \end{aligned}$$

We can see that the other term in Eq. (8) is negligible. Using $P_{\text{ie}(\sigma_*) - 1} = \Theta(1/\rho)$, plugging this result into Eq. (7) yields

$$\begin{aligned} & \mathbb{E}_{\mathbf{x}}[y \alpha L_m \{ \sqrt{r}\Gamma^* \mathbf{x} \cdot \gamma(\mathbf{x}, y) \langle \beta^*, \mathbf{u} \rangle + \sqrt{r}\Gamma^* \gamma(\mathbf{x}, y) \langle \mathbf{x}, \mathbf{u} \rangle \beta^* \}] \\ &= \alpha L_m \langle \beta, \mathbf{u} \rangle \frac{\beta}{\kappa^{\text{ie}(\sigma_*) + 1} \rho^{\text{ie}(\sigma_*)}} \{ (\kappa\sqrt{r})^{-(\text{ie}(\sigma_*) - 1)} (1 + O(1/\sqrt{d})) + \langle \beta, \mathbf{u} \rangle^{2\text{ie}(\sigma_*) - 2} (1 + O(1/\sqrt{d})) \} \end{aligned}$$

with high probability. Finally, we evaluate the term $\mathbb{E}_{\mathbf{x}}[\alpha L_m \sigma_*(\langle \beta, \mathbf{x} \rangle)(\sqrt{r}\Gamma^* \mathbf{x} \cdot \mathbf{n}_1 + \langle \mathbf{x}, \mathbf{u} \rangle \mathbf{n}_2)]$. From Corollary 17 of [Oko et al. \(2024\)](#), we have $\sigma_*(\langle \beta, \mathbf{x} \rangle) = O_p(\log^{\text{deg}(\sigma_*)/2} d)$. Moreover, from Lemma C.1, it holds that $\mathbf{n}_1 = \tilde{O}(C_u \sqrt{\frac{1}{N_1}})$ and $\mathbf{n}_2 = \tilde{O}(\sqrt{\frac{r}{N_1}})$ with high probability. Therefore, we arrive at

$$\mathbb{E}_{\mathbf{x}}[\alpha L_m \sigma_*(\langle \beta, \mathbf{x} \rangle)(\sqrt{r}\Gamma^* \mathbf{x} \cdot \mathbf{n}_1 + \langle \mathbf{x}, \mathbf{u} \rangle \mathbf{n}_2)] = \tilde{O}_p \left(\alpha m C_u \sqrt{\frac{r}{N_1}} \right).$$

Combining all results above completes the proof. \square

The following lemma will be useful in the analysis of weak recovery (the next section).

Lemma C.3. *When $\text{ge}(\sigma_*) = 2$, $\gamma(\mathbf{x}, y) = \tilde{O}(1/\sqrt{r})$ holds with high probability.*

Proof. Recall that

$$\begin{aligned} \gamma(\mathbf{x}, y) &= P_0 + P_1 z + \dots \\ &= \left(k_\rho \sum_{i \geq 0} \frac{B_i}{i!} z^i \right)^{-2} \left\{ \left[k_\rho \left(\sum_{i \geq 0} \frac{A_{i+1}}{i!} z^i \right) + k'_\rho \left(\sum_{i \geq 0} \frac{B_{i+1}}{i!} z^i \right) \right] \cdot k_\rho \left(\sum_{i \geq 0} \frac{B_i}{i!} z^i \right) \right. \\ &\quad \left. - k_\rho \left(\sum_{i \geq 0} \frac{B_{i+1}}{i!} z^i \right) \cdot \left[k_\rho \left(\sum_{i \geq 0} \frac{A_i}{i!} z^i \right) + k'_\rho \left(\sum_{i \geq 0} \frac{B_i}{i!} z^i \right) \right] \right\}. \end{aligned}$$

By expanding the RHS in powers of z and comparing their coefficients, we obtain

$$\begin{aligned} P_0 &= \frac{(k_\rho A_0 + k'_\rho B_0) \cdot k_\rho B_1 - k_\rho B_0 (k_\rho A_1 + k'_\rho B_1)}{(k_\rho B_0)^2} \\ &= \frac{A_0 B_1 - B_0 A_1}{B_0^2}. \end{aligned}$$

When $\text{ge}(\sigma_*)$ is 2, σ_* is even, and thus $\exp(\bar{\sigma}_*)$ and $\bar{\sigma}_* \exp(\bar{\sigma}_*)$ are also even. This means that $\exp(\bar{\sigma}_*)$ and $\bar{\sigma}_* \exp(\bar{\sigma}_*)$ can be expanded in polynomial of z^2 . This means that the coefficients of z in the hermite expansion of $\exp(\bar{\sigma}_*)$ and $\bar{\sigma}_* \exp(\bar{\sigma}_*)$ are 0, namely $A_1 = B_1 = 0$, which yields $P_0 = 0$. Hence, we have

$$\gamma(\mathbf{x}, y) = P_1 z + P_2 z^2 + \dots,$$

where $P_1 = \tilde{O}(1)$ and $z = \tilde{O}_p(1/\sqrt{r})$, which yields the assertion. \square

D. One step gradient descent for weak recovery

Lemma D.1. *Set $C_u = 1/\sqrt{r}$, $N_1 = \tilde{\Omega}(r^{\text{ge}(\sigma_*)+1})$ and $N_{new} = \tilde{\Omega}(r^{\text{ge}(\sigma_*)+2})$. Let $w_i \stackrel{i.i.d.}{\sim} \mathcal{N}(0, \mathbf{I}_d)$ for $i = 1, 2, \dots, N_{new}$ and $\mathbf{h} = \frac{1}{2} \sqrt{r} \Gamma^* \frac{1}{N_{new}} \sum_{i=1}^{N_{new}} \nabla_{\mathbf{u}} (f_{\text{IC}}(\mathbf{w}_i) - (g(\Gamma^*, \mathbf{w}_i) - b))^2$, then*

$$\begin{aligned} \mathbf{h} &= P'_2 \Theta(\alpha_1 m) \langle \beta, \mathbf{u} \rangle \frac{\beta}{\kappa^{2\text{ge}(\sigma_*)} \rho^{\text{ge}(\sigma_*)}} (\sqrt{r})^{-(2\text{ge}(\sigma_*)-1)} (1 + O(1/\sqrt{d})) \\ &\quad + \tilde{O}(\alpha_1^2 m^2 r^{-1/2} r^{-\frac{\text{ge}(\sigma_*)-1}{2}}) + \tilde{O} \left(\alpha_1 m \sqrt{\frac{r^{-\text{ge}(\sigma_*)}}{N_1}} \right) + \tilde{O} \left(\alpha_1 m \sqrt{\frac{r^{-\text{ge}(\sigma_*)}}{N_{new}}} \right) + \tilde{O}(\alpha_1 m r^{-\text{ge}(\sigma_*)-1/2}) \end{aligned}$$

holds with high probability.

Proof. From Lemma B.1, we have that

$$g(\Gamma^*, \mathbf{x}) = P'_1 + P'_2 \left(\frac{\langle \mathbf{x}, \beta \rangle}{\sqrt{r}} \right)^{\text{ge}(\sigma_*)} + n_3,$$

where $P'_1 = o_d(1)$, $P'_2 = \Theta_d((\log d)^{-C_{P_2}})$ and $n_3 = o_d(P'_2 r^{-\text{ge}(\sigma_*)/2-1/2} \log^{-2 \deg(\sigma_*)+2} d)$. Noticing that $g(\Gamma^*, \mathbf{x}) = O(1)$ with high probability, then, letting $b = \frac{1}{N_{new}} \sum_{i=1}^{N_{new}} g(\Gamma^*, \mathbf{w}_i)$ and applying Lemma H.2, it holds that

$$g(\Gamma^*, \mathbf{w}_i) - b = P'_2 r^{-\frac{\text{ge}(\sigma_*)}{2}} \text{He}_{\text{ge}(\sigma_*)}(\langle \beta, \mathbf{w}_i \rangle) + n_3 + \tilde{O}(1/\sqrt{N_{new}}).$$

When $N_{new} = O(r^{\text{ge}(\sigma_*)+2})$, the term $\tilde{O}(1/\sqrt{N_{new}})$ can be dominated by n_3 , which means that

$$g(\Gamma^*, \mathbf{w}_i) - b = P'_2 r^{-\frac{\text{ge}(\sigma_*)}{2}} \text{He}_{\text{ge}(\sigma_*)}(\langle \beta, \mathbf{w}_i \rangle) + n_3,$$

and $n_3 = o_d(P'_2 r^{-\text{ge}(\sigma_*)/2-1/2} \log^{-2 \text{deg}(\sigma_*)+2} d)$ with high probability.

In this stage, we use $g(\Gamma^*, \mathbf{w}_i) - b$ as a teacher signal. Thus, as $C_u = 1/\sqrt{r}$ and $g(\Gamma^*, \mathbf{w}_i) - b = \tilde{O}(r^{-\frac{\text{ge}(\sigma_*)}{2}})$, with high probability, we have

$$\begin{aligned} & \frac{1}{2} \sqrt{r} \Gamma^* \nabla_{\mathbf{u}} (f_{\text{IC}}(\mathbf{w}_i) - (g(\Gamma^*, \mathbf{w}_i) - b))^2 \\ &= \tilde{O}(\alpha_1^2 m^2 r^{-1/2} r^{-\frac{\text{ge}(\sigma_*)-1}{2}}) - \left\{ P'_2 r^{-\frac{\text{ge}(\sigma_*)}{2}} \text{He}_{\text{ge}(\sigma_*)}(\langle \beta, \mathbf{w}_i \rangle) + n_3 \right\} \cdot \sqrt{r} \Gamma^* \nabla_{\mathbf{u}} f_{\text{IC}}(\mathbf{w}_i). \end{aligned}$$

Following the same argument as Lemma 3.2 yields

$$\begin{aligned} & P'_2 r^{-\frac{\text{ge}(\sigma_*)}{2}} \text{He}_{\text{ge}(\sigma_*)}(\langle \beta, \mathbf{w}_i \rangle) \cdot \sqrt{r} \Gamma^* \nabla_{\mathbf{u}} f_{\text{IC}}(\mathbf{w}_i) \\ &= P'_2 \Theta(\alpha_1 m) \langle \beta, \mathbf{u} \rangle \frac{r^{-\frac{\text{ge}(\sigma_*)}{2}} \beta}{\kappa^{\text{ge}(\sigma_*)+1} \rho^{\text{ge}(\sigma_*)}} \left\{ (\kappa \sqrt{r})^{-(\text{ge}(\sigma_*)-1)} (1 + O(1/\sqrt{d})) + \langle \beta, \mathbf{u} \rangle^{2\text{ge}(\sigma_*)-2} (1 + O(1/\sqrt{d})) \right\} \\ & \quad + \nu + \tilde{O} \left(\alpha_1 m \sqrt{\frac{r^{-\text{ge}(\sigma_*)}}{N_1}} \right) \end{aligned}$$

with high probability. Since $\langle \beta, \mathbf{u} \rangle = \tilde{O}_p(1/r)$ at the initialization, the first term (regarding $(\kappa \sqrt{r})^{-(\text{ge}(\sigma_*)-1)}$) dominates the second term (regarding $\langle \beta, \mathbf{u} \rangle^{2\text{ge}(\sigma_*)-2}$). Taking the average over $i = 1, \dots, N_{\text{new}}$ yields that

$$\begin{aligned} & P'_2 r^{-\frac{\text{ge}(\sigma_*)}{2}} \frac{1}{N_{\text{new}}} \sum_{i=1}^{N_{\text{new}}} \text{He}_{\text{ge}(\sigma_*)}(\langle \beta, \mathbf{w}_i \rangle) \cdot \sqrt{r} \Gamma^* \nabla_{\mathbf{u}} f_{\text{IC}}(\mathbf{w}_i) \\ &= P'_2 \Theta(\alpha_1 m) \langle \beta, \mathbf{u} \rangle \frac{\beta}{\kappa^{2\text{ge}(\sigma_*)} \rho^{\text{ge}(\sigma_*)}} (\sqrt{r})^{-(2\text{ge}(\sigma_*)-1)} (1 + O(1/\sqrt{d})) \\ & \quad + \frac{1}{N_{\text{new}}} \sum_{i=1}^{N_{\text{new}}} \nu_i + \tilde{O} \left(\alpha_1 m \sqrt{\frac{r^{-\text{ge}(\sigma_*)}}{N_1}} \right), \end{aligned}$$

where ν_i is a series of i.i.d. mean-zero random variable vectors which satisfy $\nu_i = \tilde{O}_p(\alpha_1 m \cdot r^{-\text{ge}(\sigma_*)/2})$. Then, from Hoeffding's inequality, we have

$$\frac{1}{N_{\text{new}}} \sum_{i=1}^{N_{\text{new}}} \nu_i = \tilde{O} \left(\alpha_1 m \sqrt{\frac{r^{-\text{ge}(\sigma_*)}}{N_{\text{new}}}} \right),$$

with high probability. Next we investigate the effect of n_3 . From Lemma C.1, $\sqrt{r} \Gamma^* \nabla_{\mathbf{u}} f_{\text{IC}}(\mathbf{w}_i) = \tilde{O}(\alpha_1 m C_u) = \tilde{O}(\alpha_1 m r^{-1/2})$ holds. This leads to $n_3 \sqrt{r} \Gamma^* \nabla_{\mathbf{u}} f_{\text{IC}}(\mathbf{w}_i) = \tilde{O}(\alpha_1 m r^{-\text{ge}(\sigma_*)/2-1/2})$. Moreover, from Lemma C.3, when $\text{ge}(\sigma_*) = 2$ we have $\gamma(\mathbf{x}, \mathbf{y}) = O(1/\sqrt{r})$. Combining this fact with $N_1 = \tilde{\Omega}(r^{\text{ge}(\sigma_*)+1})$ yields $\sqrt{r} \Gamma^* \nabla_{\mathbf{u}} f_{\text{IC}}(\mathbf{w}_i) = \tilde{O}(\alpha_1 m/r)$. Therefore, whether $\text{ge}(\sigma_*) = 1$ or $\text{ge}(\sigma_*) = 2$, we obtain

$$n_3 \sqrt{r} \Gamma^* \nabla_{\mathbf{u}} f_{\text{IC}}(\mathbf{w}_i) = \tilde{O}(\alpha_1 m r^{-\text{ge}(\sigma_*)-1/2}).$$

Taking the average over $i = 1, \dots, N_{\text{new}}$ completes the proof. \square

Lemma D.2. *Under the condition of Lemma D.1, it holds that*

$$\begin{aligned} \langle \beta, \mathbf{h} \rangle &= P'_2 \Theta(\alpha_1 m) \langle \beta, \mathbf{u} \rangle \frac{1}{\kappa^{2\text{ge}(\sigma_*)} \rho^{\text{ge}(\sigma_*)}} (\sqrt{r})^{-(2\text{ge}(\sigma_*)-1)} (1 + O(1/\sqrt{d})) \\ & \quad + \tilde{O} \left(\alpha_1^2 m^2 r^{-\frac{\text{ge}(\sigma_*)}{2}} \right) + \tilde{O} \left(\alpha_1 m \sqrt{\frac{r^{-\text{ge}(\sigma_*)}}{N_1}} \right) + \tilde{O} \left(\alpha_1 m \sqrt{\frac{r^{-\text{ge}(\sigma_*)}}{N_{\text{new}}}} \right) + o(\alpha_1 m r^{-\text{ge}(\sigma_*)-1/2}), \end{aligned}$$

with high probability.

Proof. As $\|\beta\| = 1$, using the result of Lemma D.1 and taking the inner product of \mathbf{h} and β yields

$$\begin{aligned} \langle \beta, \mathbf{h} \rangle &= P'_2 \Theta(\alpha_1 m) \langle \beta, \mathbf{u} \rangle \frac{1}{\kappa^{2\text{ge}(\sigma_*)} \rho^{\text{ge}(\sigma_*)}} (\sqrt{r})^{-(2\text{ge}(\sigma_*)-1)} (1 + O(1/\sqrt{d})) \\ &\quad + \tilde{O}(\alpha_1^2 m^2 r^{-\frac{\text{ge}(\sigma_*)}{2}}) + \tilde{O}\left(\alpha_1 m \sqrt{\frac{r^{-\text{ge}(\sigma_*)}}{N_1}}\right) + \tilde{O}\left(\alpha_1 m \sqrt{\frac{r^{-\text{ge}(\sigma_*)}}{N_{\text{new}}}}\right) + \tilde{O}\left(\alpha_1 m r^{-\text{ge}(\sigma_*)-1/2}\right). \end{aligned}$$

However, by carefully investigating the last term ($\tilde{O}(\alpha_1 m r^{-\text{ge}(\sigma_*)-1/2})$) in the RHS, we can obtain a tighter bound of that term. Indeed, this term arises from

$$\begin{aligned} &n_3 \left\langle \beta, \frac{1}{N_{\text{new}}} \sum_{i=1}^{N_{\text{new}}} \sqrt{r} \Gamma^* \nabla_{\mathbf{u}} f_{\text{IC}}(\mathbf{w}_i) \right\rangle \\ &= n_3 \alpha_1 L_m \frac{1}{N_{\text{new}}} \sum_{i=1}^{N_{\text{new}}} \left\{ \langle \beta, \sqrt{r} \Gamma^* \mathbf{x} \rangle \cdot \gamma(\mathbf{x}, y) \langle \beta^*, \mathbf{u} \rangle + \gamma(\mathbf{x}, y) \langle \mathbf{x}, \mathbf{u} \rangle \langle \beta^*, \sqrt{r} \Gamma^* \beta \rangle \right. \\ &\quad \left. + \langle \beta, \sqrt{r} \Gamma^* \mathbf{x} \rangle \cdot n_1 + \langle \mathbf{x}, \mathbf{u} \rangle \langle \beta, \mathbf{n}_2 \rangle \right\}. \end{aligned}$$

We notice that the leading term of the right hand side is $n_3 \alpha_1 L_m P_0 \langle \mathbf{u}, \mathbf{x} \rangle$ when $\text{ge}(\sigma_*) = 1$, and $n_3 \alpha_1 m P_1 \langle \beta, \sqrt{r} \Gamma_u^\top \Gamma_u \mathbf{x} \rangle / \rho \cdot \langle \mathbf{x}, \mathbf{u} \rangle$ when $\text{ge}(\sigma_*) = 2$. Note that $\mathbb{E}_{\mathbf{x}}[P_0 \langle \mathbf{u}, \mathbf{x} \rangle] = 0$ and $\mathbb{E}_{\mathbf{x}}[P_1 \langle \sqrt{r} \Gamma_u^\top \Gamma_u \beta, \mathbf{x} \rangle / \rho \cdot \langle \mathbf{x}, \mathbf{u} \rangle] = P_1 \langle \sqrt{r} \Gamma_u^\top \Gamma_u \beta, \mathbf{u} \rangle / \rho = \tilde{O}(r^{-3/2})$ because of $\sqrt{r} \Gamma_u^\top \Gamma_u \beta = \tilde{O}(1/\sqrt{r})\beta + \tilde{O}(1/r) + \langle \beta, \mathbf{u} \rangle \mathbf{u}$ (see Lemma H.8). Moreover, we have $\mathbb{E}_{\mathbf{x}}[P_0^2 \langle \mathbf{u}, \mathbf{x} \rangle^2] = \tilde{O}(1)$ and $\mathbb{E}_{\mathbf{x}}[P_1^2 \langle \sqrt{r} \Gamma_u^\top \Gamma_u \beta, \mathbf{x} \rangle^2 / \rho^2 \cdot \langle \mathbf{x}, \mathbf{u} \rangle^2] \leq P_1^2 / \rho^2 \cdot \mathbb{E}[\langle \sqrt{r} \Gamma_u^\top \Gamma_u \beta, \mathbf{x} \rangle^4]^{1/2} \mathbb{E}[\langle \mathbf{x}, \mathbf{u} \rangle^4]^{1/2} = \tilde{O}(1)$. Therefore, Lemma H.2 yields that

$$\begin{aligned} \frac{1}{N_{\text{new}}} \sum_{i=1}^{N_{\text{new}}} P_0 \langle \mathbf{u}, \mathbf{w}_i \rangle &= \tilde{O}\left(\sqrt{\frac{1}{r N_{\text{new}}}}\right), \\ \frac{1}{N_{\text{new}}} \sum_{i=1}^{N_{\text{new}}} P_1 \langle \beta, \sqrt{r} \Gamma_u \Gamma_u^* \mathbf{w}_i \rangle / \rho \langle \mathbf{w}_i, \mathbf{u} \rangle &= \tilde{O}(r^{-3/2}) + \tilde{O}(r^{-1} N_{\text{new}}^{-1/2}). \end{aligned}$$

Since $n_3 = o_d(P'_2 r^{-\text{ge}(\sigma_*)/2-1/2} \log^{-2 \text{deg}(\sigma_*)+2} d)$ and $N_{\text{new}} = \tilde{\Omega}(r^{\text{ge}(\sigma_*)+2})$, this implies that

$$n_3 \left\langle \beta, \frac{1}{N_{\text{new}}} \sum_{i=1}^{N_{\text{new}}} \sqrt{r} \Gamma^* \nabla_{\mathbf{u}} f_{\text{IC}}(\mathbf{w}_i) \right\rangle = o(\alpha_1 m r^{-\text{ge}(\sigma_*)-1/2}).$$

This yields the assertion. \square

Setting the parameters directly yields the following lemma:

Lemma D.3. *Set $N_1 = \tilde{\Omega}(r^{\text{ge}(\sigma_*)+2})$, $N_{\text{new}} = \tilde{\Omega}(r^{\text{ge}(\sigma_*)+2})$, $\alpha_1 m = \tilde{\Theta}(r^{-\text{ge}(\sigma_*)/2-1})$, $\eta_1 = \tilde{\Theta}(r^{3\text{ge}(\sigma_*)/2+3/2})$ and $\lambda_1 = \eta_1^{-1}$, then we have*

$$\mathbf{u}^1 = \tilde{\Theta}(1)\beta + \tilde{O}(1),$$

and

$$\langle \beta, \mathbf{u}^1 \rangle = \tilde{\Theta}(1) + o(1),$$

with high probability. In particular, we have that

$$\left\langle \beta, \frac{\mathbf{u}^1}{\|\mathbf{u}^1\|} \right\rangle \geq 1/\text{polylog}(d).$$

E. Strong recovery

After achieving weak recovery, we train the vector \mathbf{u} , regarding the in-context examples (x_i, y_i) as training data. The idea of proof in this section is taken from Lee et al. (2024), but we achieve better sample complexity.

Lemma E.1. Let $\mathbf{h} = \frac{1}{2}\sqrt{r}\Gamma^*\nabla_{\mathbf{u}}(f_{\text{IC}}(\mathbf{x}) - y)^2$. Then, we have that

$$\begin{aligned}\mathbf{h} &= \Theta(\alpha_2 m) \langle \beta, \mathbf{u} \rangle^{2\text{ie}(\sigma_*)-1} \frac{\beta}{\kappa^{\text{ie}(\sigma_*)+1} \rho^{\text{ie}(\sigma_*)}} (1 + O(1/\sqrt{d})) \\ &\quad + \tilde{O}(\alpha_2^2 m^2 \sqrt{r}) + \tilde{O}\left(\alpha_2 m \sqrt{\frac{r}{N_2}}\right) + \nu, \\ \langle \beta, \mathbf{h} \rangle &= \Theta(\alpha_2 m) \langle \beta, \mathbf{u} \rangle^{2\text{ie}(\sigma_*)-1} \frac{1}{\kappa^{\text{ie}(\sigma_*)+1} \rho^{\text{ie}(\sigma_*)}} (1 + O(1/\sqrt{d})) \\ &\quad + \tilde{O}(\alpha_2^2 m^2 \sqrt{r}) + \tilde{O}\left(\alpha_2 m \sqrt{\frac{r}{N_2}}\right) + \nu_6, \\ \langle \mathbf{u}, \mathbf{h} \rangle &= \Theta(\alpha_2 m) \langle \beta, \mathbf{u} \rangle^{2\text{ie}(\sigma_*)} \frac{1}{\kappa^{\text{ie}(\sigma_*)+1} \rho^{\text{ie}(\sigma_*)}} (1 + O(1/\sqrt{d})) \\ &\quad + \tilde{O}(\alpha_2^2 m^2 \sqrt{r}) + \tilde{O}\left(\alpha_2 m \sqrt{\frac{r}{N_2}}\right) + \nu_7,\end{aligned}$$

with high probability, where ν_6 and ν_7 are mean-zero sub-Weibull random variables. Moreover, $\nu_6 = \tilde{O}(\alpha_2 m)$ and $\nu_7 = \tilde{O}(\alpha_2 m)$ hold with high probability.

Proof. Remember that, in the stage of strong recovery, the initialization scale is α_2 , the context length is N_2 and $C_u = 1$. By using the same argument to derive Lemma 3.2, we have

$$\begin{aligned}\mathbf{h} &= \Theta(\alpha_2 m) \langle \beta, \mathbf{u} \rangle \frac{\beta}{\kappa^{\text{ie}(\sigma_*)+1} \rho^{\text{ie}(\sigma_*)}} \{(\kappa\sqrt{r})^{-(\text{ie}(\sigma_*)-1)} (1 + O(1/\sqrt{d})) + \langle \beta, \mathbf{u} \rangle^{2\text{ie}(\sigma_*)-2} (1 + O(1/\sqrt{d}))\} \\ &\quad + \tilde{O}(\alpha_2^2 m^2 \sqrt{r}) + \tilde{O}\left(\alpha_2 m \sqrt{\frac{r}{N_2}}\right) + \nu.\end{aligned}$$

Now, since $\langle \beta, \mathbf{u} \rangle \geq 1/\text{polylog}(d)$, the term $\langle \beta, \mathbf{u} \rangle^{2\text{ie}(\sigma_*)-2}$ dominates over the term $(\kappa\sqrt{r})^{-(\text{ie}(\sigma_*)-1)}$. Therefore, with high probability, we have

$$\begin{aligned}\mathbf{h} &= \Theta(\alpha_2 m) \langle \beta, \mathbf{u} \rangle^{2\text{ie}(\sigma_*)-1} \frac{\beta}{\kappa^{\text{ie}(\sigma_*)+1} \rho^{\text{ie}(\sigma_*)}} (1 + O(1/\sqrt{d})) \\ &\quad + \tilde{O}(\alpha_2^2 m^2 \sqrt{r}) + \tilde{O}\left(\alpha_2 m \sqrt{\frac{r}{N_2}}\right) + \nu.\end{aligned}$$

Next, since $\|\beta\| = 1$, we have

$$\begin{aligned}\langle \beta, \mathbf{h} \rangle &= \Theta(\alpha_2 m) \langle \beta, \mathbf{u} \rangle^{2\text{ie}(\sigma_*)-1} \frac{1}{\kappa^{\text{ie}(\sigma_*)+1} \rho^{\text{ie}(\sigma_*)}} (1 + O(1/\sqrt{d})) \\ &\quad + \tilde{O}(\alpha_2^2 m^2 \sqrt{r}) + \tilde{O}\left(\alpha_2 m \sqrt{\frac{r}{N_2}}\right) + \langle \nu, \beta \rangle,\end{aligned}$$

with high probability, where $\nu = \tilde{O}(\alpha_2 m \sqrt{r})$. Then, since we see that

$$\begin{aligned}\nu &= y \cdot \alpha_2 L_m \left\{ \sqrt{r}\Gamma^* \mathbf{x} \cdot \gamma(\mathbf{x}, y) \langle \beta^*, \mathbf{u} \rangle + \sqrt{r}\Gamma^* \gamma(\mathbf{x}, y) \langle \mathbf{x}, \mathbf{u} \rangle \beta^* + \sqrt{r}\Gamma^* \mathbf{x} \cdot \mathbf{n}_1 + \langle \mathbf{x}, \mathbf{u} \rangle \mathbf{n}_2 \right\} \\ &\quad - \mathbb{E}_{\mathbf{x}}[y \cdot \alpha_2 L_m \left\{ \sqrt{r}\Gamma^* \mathbf{x} \cdot (\gamma(\mathbf{x}, y) \langle \beta^*, \mathbf{u} \rangle + \sqrt{r}\Gamma^* \gamma(\mathbf{x}, y) \langle \mathbf{x}, \mathbf{u} \rangle \beta^* + \sqrt{r}\Gamma^* \mathbf{x} \cdot \mathbf{n}_1 + \langle \mathbf{x}, \mathbf{u} \rangle \mathbf{n}_2) \right\}],\end{aligned}$$

it holds that

$$\begin{aligned}&\langle \beta, \nu \rangle \\ &= y \cdot \alpha_2 L_m \left\{ \langle \beta, \sqrt{r}\Gamma^* \mathbf{x} \rangle \cdot \gamma(\mathbf{x}, y) \langle \beta^*, \mathbf{u} \rangle + \gamma(\mathbf{x}, y) \langle \mathbf{x}, \mathbf{u} \rangle \langle \beta, \sqrt{r}\Gamma^* \beta^* \rangle + \langle \beta, \sqrt{r}\Gamma^* \mathbf{x} \rangle \cdot \mathbf{n}_1 + \langle \mathbf{x}, \mathbf{u} \rangle \langle \beta, \mathbf{n}_2 \rangle \right\} \\ &\quad - \mathbb{E}_{\mathbf{x}}[y \cdot \alpha_2 L_m \left\{ \langle \beta, \sqrt{r}\Gamma^* \mathbf{x} \rangle \cdot \gamma(\mathbf{x}, y) \langle \beta^*, \mathbf{u} \rangle + \gamma(\mathbf{x}, y) \langle \mathbf{x}, \mathbf{u} \rangle \langle \beta, \sqrt{r}\Gamma^* \beta^* \rangle + \langle \beta, \sqrt{r}\Gamma^* \mathbf{x} \rangle \cdot \mathbf{n}_1 + \langle \mathbf{x}, \mathbf{u} \rangle \langle \beta, \mathbf{n}_2 \rangle \right\}].\end{aligned}$$

Here, the first term of the right hand side satisfies

$$\begin{aligned} & y \cdot \alpha_2 L_m \left\{ \langle \beta, \sqrt{r} \Gamma^* \mathbf{x} \rangle \cdot \gamma(\mathbf{x}, y) \langle \beta^*, \mathbf{u} \rangle + \gamma(\mathbf{x}, y) \langle \mathbf{x}, \mathbf{u} \rangle \langle \beta, \sqrt{r} \Gamma^* \beta^* \rangle \right. \\ & \quad \left. + \langle \beta, \sqrt{r} \Gamma^* \mathbf{x} \rangle \cdot n_1 + \langle \mathbf{x}, \mathbf{u} \rangle \langle \beta, \mathbf{n}_2 \rangle \right\} \\ & = \tilde{O}(\alpha_2 m), \end{aligned}$$

with high probability, and $\langle \beta, \nu \rangle$ is the difference between this random variable and its expectation. Thus, by defining $\nu_6 = \langle \beta, \nu \rangle$, Hoeffding's inequality yields that $\nu_6 = \tilde{O}(\alpha_2 m)$ with high probability. Moreover, since $|\langle \beta, \nu \rangle| \leq \|\nu\|$, $\nu_6 = \langle \beta, \nu \rangle$ has sub-Weibull tail.

Likewise, we have that

$$\begin{aligned} \langle \mathbf{u}, \mathbf{h} \rangle & = \Theta(\alpha_2 m) \langle \beta, \mathbf{u} \rangle^{2ie(\sigma_*)} \frac{1}{\kappa^{ie(\sigma_*)+1} \rho^{ie(\sigma_*)}} (1 + O(1/\sqrt{d})) \\ & \quad + \tilde{O}(\alpha_2^2 m^2 \sqrt{r}) + \tilde{O}\left(\alpha_2 m \sqrt{\frac{r}{N_2}}\right) + \nu_7, \end{aligned}$$

where ν_7 is a mean-zero sub-Weibull random variable satisfying $\nu_7 = \tilde{O}(\alpha_2 m)$. \square

Lemma E.2. *Let $a^{(n)} = \langle \beta, \mathbf{u}^{(n)} \rangle$. Suppose that $c_1 \leq a^{(n)} \leq 1 - \varepsilon$ where $c_1 = \tilde{\Theta}(1)$. Set $\alpha_2 m = \tilde{\Theta}(\varepsilon/r)$, $N_2 = \tilde{\Theta}(r^2)$ and $\eta_2 = \tilde{\Theta}(1/\sqrt{r})$. Then, there exists $c_3 = \tilde{\Theta}(1)$ which satisfies*

$$a^{(n+1)} \geq a^{(n)} + \frac{c_3 \varepsilon}{r \sqrt{r}} a^{(n)2ie(\sigma_*)-1} (1 - a^{(n)2}) (1 - O(1/\sqrt{d})) + \nu_8 - \tilde{O}(\varepsilon/r^2),$$

with high probability, where ν_8 is a mean-zero sub-Weibull random variable which satisfies $\nu_8 = \tilde{O}(\varepsilon/r\sqrt{r})$ with high probability.

Proof. Using the projection matrix $\mathbf{P}_u = \mathbf{I} - uu^\top$, online SGD update can be written as

$$\mathbf{u}^{(n+1)} = \mathbf{u}^{(n)} + \frac{\mathbf{u}^{(n)} + \eta_2 \mathbf{P}_{\mathbf{u}^{(n)}} \mathbf{h}}{\|\mathbf{u}^{(n)} + \eta_2 \mathbf{P}_{\mathbf{u}^{(n)}} \mathbf{h}\|},$$

which gives

$$\begin{aligned} & \langle \beta, \mathbf{u}^{(n+1)} \rangle \\ & = \langle \beta, \mathbf{u}^{(n)} \rangle + \left\langle \beta, \frac{\mathbf{u}^{(n)} + \eta_2 \mathbf{P}_{\mathbf{u}^{(n)}} \mathbf{h}}{\|\mathbf{u}^{(n)} + \eta_2 \mathbf{P}_{\mathbf{u}^{(n)}} \mathbf{h}\|} \right\rangle \\ & = \langle \beta, \mathbf{u}^{(n)} \rangle + \eta_2 \langle \beta, \mathbf{P}_{\mathbf{u}^{(n)}} \mathbf{h} \rangle - \frac{1}{2} \eta_2^2 \|\mathbf{P}_{\mathbf{u}^{(n)}} \mathbf{h}\|^2 + O(\eta_2^3) \\ & = \langle \beta, \mathbf{u}^{(n)} \rangle + \eta_2 \langle \beta, \mathbf{h} \rangle - \eta_2 \langle \beta, \mathbf{u}^{(n)} \rangle \langle \mathbf{u}^{(n)}, \mathbf{h} \rangle - \frac{1}{2} \eta_2^2 \|\mathbf{P}_{\mathbf{u}^{(n)}} \mathbf{h}\|^2 + O((\eta_2 \|\mathbf{h}\|)^3). \end{aligned}$$

By the definition of $a^{(n)}$, i.e., $a^{(n)} = \langle \beta, \mathbf{u}^{(n)} \rangle$, we have

$$a^{(n+1)} = a^{(n)} + \eta_2 \langle \beta, \mathbf{h} \rangle - \eta_2 a^{(n)} \langle \mathbf{u}^{(n)}, \mathbf{h} \rangle - \frac{1}{2} \eta_2^2 \|\mathbf{P}_{\mathbf{u}^{(n)}} \mathbf{h}\|^2 + O((\eta_2 \|\mathbf{h}\|)^3).$$

Now, from Lemma E.1, we also have

$$\langle \beta, \mathbf{h} \rangle = \frac{\varepsilon}{r} a^{(n)2ie(\sigma_*)-1} (\tilde{\Theta}(1) + O(1/\sqrt{d})) + \tilde{O}(\varepsilon/r\sqrt{r}) + \tilde{O}(\varepsilon/r\sqrt{r}) + \nu_6$$

and

$$\langle \mathbf{u}, \mathbf{h} \rangle = \frac{\varepsilon}{r} a^{(n)2ie(\sigma_*)} (\tilde{\Theta}(1) + O(1/\sqrt{d})) + \tilde{O}(\varepsilon/r\sqrt{r}) + \tilde{O}(\varepsilon/r\sqrt{r}) + \nu_7.$$

Moreover, since $\|\mathbf{P}_{u^{(n)}} \mathbf{h}\| = \tilde{O}(\alpha_2 m \sqrt{r}) = \tilde{O}(\varepsilon/\sqrt{r})$, it holds that

$$\frac{1}{2} \eta_2^2 \|\mathbf{P}_{u^{(n)}} \mathbf{h}\|^2 = \tilde{O}(\varepsilon^2/r^2).$$

Therefore, ignoring the term $O((\eta_2 \|\mathbf{h}\|)^3)$, we arrive at

$$\begin{aligned} a^{(n+1)} &= a^{(n)} + \eta_2 \langle \beta, \mathbf{h} \rangle - \eta_2 a^{(n)} \langle \mathbf{u}, \mathbf{h} \rangle - \frac{1}{2} \eta_2^2 \|\mathbf{P}_{u^{(n)}} \mathbf{h}\|^2 \\ &= a^{(n)} + \frac{\eta_2 \varepsilon}{r} a^{(n) 2ie(\sigma_*)-1} (1 - a^{(n)2}) (\tilde{\Theta}(1) + O(1/\sqrt{d})) + \eta_2 (\nu_6 - a^{(n)} \nu_7) + \eta_2 \tilde{O}(\varepsilon/r\sqrt{r}) + \tilde{O}(\varepsilon/r^2) \\ &\geq a^{(n)} + \frac{c_3 \varepsilon}{r\sqrt{r}} a^{(n) 2ie(\sigma_*)-1} (1 - a^{(n)2}) (1 - O(1/\sqrt{d})) + \nu_8 - \tilde{O}(\varepsilon/r^2), \end{aligned}$$

where ν_8 is a mean-zero sub-Weibull random variable satisfying $\nu_8 = \tilde{O}(\varepsilon/r\sqrt{r})$. \square

Lemma E.3. Suppose that $\mathbf{u}^{(1)}$ satisfies $\langle \beta, \mathbf{u}^{(1)} \rangle \geq c_1$, where $c_1 \geq 1/\text{polylog}(d)$. Then, there exists $N_3 = \tilde{\Theta}(\frac{r\sqrt{r}}{\varepsilon} \log \frac{1}{\varepsilon})$ such that

$$\langle \beta, \mathbf{u}^{(N_3+1)} \rangle \geq 1 - \varepsilon$$

with high probability.

Proof. Before going into the proof, we first explain the main idea of the proof. Following the same argument as Lemma 19 in Lee et al. (2024), we can see that after $\tilde{\Theta}(r\sqrt{r}/\varepsilon)$ steps, $a^{(n)}$ becomes larger than a constant $\sqrt{\frac{k+1}{k+2}}$, where $k = 2ie(\sigma_*) - 1$. Then, by applying the Mean Value theorem, we can observe that $1 - a^{(i+1)} \lesssim (1 - \frac{c_3 \varepsilon}{r\sqrt{r}} C_k) (1 - a^{(i)})$ where $C_k = \Theta(1)$. This means $1 - a^{(i)}$ converges to 0 geometrically, which yields the required data length $N_3 = \tilde{\Theta}(\frac{r\sqrt{r}}{\varepsilon} \log \frac{1}{\varepsilon})$.

Let $\nu_9^{(i)} = r\sqrt{r}\nu_8^{(i)}/\varepsilon$ and $k = 2ie(\sigma_*) - 1$. Because $\nu_9^{(i)}$ is a sequence of mean-zero sub-Weibull random variables with $\nu_9^{(i)} = \tilde{O}_p(1)$, we have

$$\left| \sum_{i=j}^{j+l} \nu_9^{(i)} \right| = C\sqrt{l}, \quad (9)$$

for any $1 \leq j, l \leq N_3$ with high probability, where $C = \tilde{O}(1)$. Let $c_k = 1 - \sqrt{\frac{k+1}{k+2}}$. Note that c_k is a constant that only depends on k , that is $c_k = O(1)$. Suppose that $c_1 \leq a^{(i)} \leq 1 - \frac{1}{3}c_k$ for all $i = 1, 2, \dots, N_3$. Then, from Lemma E.2, we have

$$a^{(n+1)} \geq a^{(n)} + \frac{c_3 \varepsilon}{r\sqrt{r}} a^{(n) 2ie(\sigma_*)-1} (1 - a^{(n)2}) (1 - O(1/\sqrt{d})) + \nu_8 - \tilde{O}(\varepsilon/r^2),$$

for $i \leq N_3$. The term $O(1/\sqrt{d})$ is smaller than 1, thus we may ignore this term. Moreover, the term $\tilde{O}(\varepsilon/r^2)$ is dominated by $\frac{c_3 \varepsilon}{r\sqrt{r}} a^{(n) 2ie(\sigma_*)-1} (1 - a^{(n)2}) = \tilde{O}(\frac{\varepsilon}{r\sqrt{r}})$. Let $c_2 = c_1^{2ie(\sigma_*)-1}$. By ignoring these terms and using $1 - a^{(i)2} \geq \frac{1}{3}c_k$, we have

$$a^{(i+1)} \geq a^{(i)} + \frac{c_2 c_3}{r\sqrt{r}} \varepsilon \cdot c_k / 3 + \frac{\varepsilon}{r\sqrt{r}} \cdot \nu_9^{(i)} \quad (10)$$

$$\geq a^{(1)} + \frac{c_2 c_3 c_k}{3r\sqrt{r}} \varepsilon i - \frac{\varepsilon}{r\sqrt{r}} \left| \sum_{j=1}^i \nu_9^{(j)} \right| \quad (11)$$

$$\geq a^{(1)} + \left(\frac{c_2 c_3 c_k}{3r\sqrt{r}} \varepsilon \right) i - \frac{\varepsilon}{r\sqrt{r}} C\sqrt{i}. \quad (12)$$

If $i \leq \frac{r^3 c_1^2}{4\varepsilon^2 C^2}$, then $\frac{\varepsilon}{r\sqrt{r}} C\sqrt{i} \leq c_1/2$, and if $i \geq (\frac{6C}{c_2 c_3 c_k})^2$, then $\frac{\varepsilon}{r\sqrt{r}} C\sqrt{i} \leq \frac{c_2 c_3 c_k}{6r\sqrt{r}} \varepsilon i$. By observing the order in terms of r , we have $\frac{r^3 c_1^2}{4\varepsilon^2 C^2} \geq (\frac{6C}{c_2 c_3 c_k})^2$ when r is sufficiently large. Therefore, it holds that

$$a^{(i+1)} \geq \frac{c_1}{2} + \frac{c_2 c_3 c_k}{6r\sqrt{r}} \varepsilon i. \quad (13)$$

When $i = \frac{6r\sqrt{r}}{c_2c_3c_k\varepsilon} = \tilde{\Theta}(r\sqrt{r}/\varepsilon)$, then the RHS of Eq. (13) exceeds 1. Therefore, there exists $i^* \leq N_3 = \tilde{\Theta}(\frac{r\sqrt{r}}{\varepsilon} \log \frac{1}{\varepsilon})$ such that $a^{(i^*)} \geq 1 - c_k/3$. Next we prove that $a^{(i)} \geq 1 - c_k = \sqrt{\frac{k+1}{k+2}}$ for all $i = i^*, i^* + 1, \dots, N_3$. In this setting, $a^{(i+1)} - a^{(i)} = \tilde{O}(\frac{\varepsilon}{r\sqrt{r}})$ holds. Therefore, if there exists $i \geq i^*$ such that $a^{(i-1)} \geq 1 - c_k/3$ and $a^{(i)} \leq 1 - c_k/3$, we have $a^{(i)} \geq 1 - 2c_k/3$ with high probability. Also, if $a^{(i+l)} \leq 1 - c_k/3$ holds for all $l = 0, 1, \dots, j-1$, we have

$$a^{(i+j)} \geq 1 - \frac{2c_k}{3} + \frac{c_2c_3c_k}{3r\sqrt{r}}\varepsilon j - \frac{\varepsilon}{r\sqrt{r}}C\sqrt{j}.$$

If $j \leq \frac{r^3c_k^2}{9\varepsilon^2C^2} = \tilde{O}(r^3/\varepsilon^2)$, then $\frac{\varepsilon}{r\sqrt{r}}C\sqrt{j} \leq c_k/3$, and if $j \geq (\frac{3C}{c_2c_3c_k})^2 = \tilde{O}(1)$, then $\frac{\varepsilon}{r\sqrt{r}}C\sqrt{j} \leq \frac{c_2c_3c_k}{3r\sqrt{r}}\varepsilon j$. Since $\frac{r^3c_k^2}{9\varepsilon^2C^2} \geq (\frac{3C}{c_2c_3c_k})^2$ when r is sufficiently large, we have

$$a^{(i+j)} \geq 1 - c_k$$

until $i+j = N_3 + 1$ or $a^{(i+j)} \geq 1 - c_k/3$ holds again. By repeating this argument if necessary, we get $a^{(i+1)} \geq 1 - c_k = \sqrt{\frac{k+1}{k+2}}$ for all $i^* \leq i \leq N_3$.

We continue by showing that, after we achieve $a^{(i^*)} \leq 1 - c_k$, the number of remaining steps needed to ensure $a^{(i)} \geq 1 - \varepsilon$ is $\tilde{O}(\frac{r\sqrt{r}}{\varepsilon} \log \frac{1}{\varepsilon})$. Let $F(x) = x + \frac{c_3\varepsilon}{r\sqrt{r}}x^k(1-x^2)$. Then,

$$a^{(i^*+i+1)} = F(a^{(i^*+i)}) + \frac{\varepsilon}{r\sqrt{r}}\nu_9^{(i^*+i)} - \tilde{O}(\varepsilon/r^2).$$

By the Mean Value theorem, there exists γ such that

$$\frac{1 - F(a^{(i^*+i)})}{1 - a^{(i^*+i)}} = F'(\gamma),$$

and $a^{(i^*+i)} < \gamma < 1$. Now $F'(x) = 1 + \frac{c_2c_3\varepsilon}{r\sqrt{r}}x^{k-1}(k - (k+2)x^2)$, and since $\gamma > a^{(i^*+i)} \geq \sqrt{\frac{k+1}{k+2}}$, we have $k - (k+2)\gamma^2 < -1$, which leads to

$$F'(\gamma) \leq 1 - \frac{c_3\varepsilon}{r\sqrt{r}}\gamma^{k-1} < 1 - \frac{c_3\varepsilon}{r\sqrt{r}}\left(\sqrt{\frac{k+1}{k+2}}\right)^{k-1}.$$

Let $C_k = \left(\sqrt{\frac{k+1}{k+2}}\right)^{k-1}$, then $1 - F(a^{(i^*+i)}) < (1 - \frac{c_3\varepsilon}{r\sqrt{r}}C_k)(1 - a^{(i^*+i)})$, which yields that

$$1 - a^{i^*+i+1} < \left(1 - \frac{c_3\varepsilon}{r\sqrt{r}}C_k\right)(1 - a^{(i^*+i)}) + \frac{\varepsilon}{r\sqrt{r}}\nu_9^{(i^*+i)} + \tilde{O}(\varepsilon/r^2).$$

Noting that $(1 - \frac{c_3\varepsilon}{r\sqrt{r}}C_k) < 1$, taking the sum leads to

$$1 - a^{(N_3+1)} < \left(1 - \frac{c_3\varepsilon}{r\sqrt{r}}C_k\right)^{N_3+1-i^*} (1 - a^{(i^*)}) + \sum_{i=i^*}^{N_3} \frac{\varepsilon}{r\sqrt{r}}\nu_9^{(i)} + \tilde{O}(\varepsilon N_3/r^2).$$

Since $\lim_{t \rightarrow \infty} (1 - \frac{1}{t})^t = 1/e$, if we set $N_3 = i^* - 1 + \frac{r\sqrt{r}}{c_3C_k\varepsilon} \log(1/\varepsilon)$, then we have

$$\begin{aligned} \left(1 - \frac{c_3\varepsilon}{r\sqrt{r}}C_k\right)^{N_3+1-i^*} (1 - a^{(i^*)}) &< \left(1 - \frac{c_3\varepsilon}{r\sqrt{r}}C_k\right)^{\frac{r\sqrt{r}}{c_3C_k\varepsilon} \log(1/\varepsilon)} \\ &\approx (1/e)^{\log(1/\varepsilon)} = \varepsilon. \end{aligned}$$

Finally, by noticing that

$$\left| \sum_{i=i^*}^{N_3} \frac{\varepsilon}{r\sqrt{r}}\nu_9^{(i)} \right| \leq \frac{\varepsilon}{r\sqrt{r}}C\sqrt{N_3 - i^* + 1} = \tilde{O}(r^{-3/4}),$$

we can see that this term is negligible. Moreover, the third term $\tilde{O}(\varepsilon N_3/r^2) = \tilde{O}(\frac{\log 1/\varepsilon}{\sqrt{r}})$ is also negligible. By summarizing the argument above, we conclude that

$$1 - a^{(N_3+1)} < \varepsilon.$$

□

In Lemma C.1, we assumed that $\langle \mathbf{u}, \mathbf{x}_i \rangle = \tilde{O}_d(1)$. Now $\mathbf{u}^{(n)}$ and \mathbf{x}_i are not independent of each other, so we need to ensure that $\langle \mathbf{u}^{(j)}, \mathbf{x}_i \rangle = \tilde{O}_d(1)$ for all $j = 1, 2, \dots, N_3 + 1$.

Lemma E.4. *It holds that*

$$\begin{aligned} \langle \mathbf{x}_i^*, \mathbf{h} \rangle &= \Theta(\alpha_2 m) \langle \beta, \mathbf{u} \rangle^{2ie(\sigma_*)-1} \frac{\langle \mathbf{x}_i^*, \beta \rangle}{(\kappa \rho)^{ie(\sigma_*)}} (1 + O(1/\sqrt{d})) \\ &\quad + \tilde{O}(\alpha_2^2 m^2 r) + \tilde{O}(\alpha_2 m r / \sqrt{N_2}) + \nu_*, \end{aligned}$$

where ν_* is a mean-zero random variable satisfying $\nu_* = \tilde{O}(\alpha_2 m \sqrt{r})$.

Proof. From Lemma E.1, we have

$$\begin{aligned} \mathbf{h} &= \Theta(\alpha_2 m) \langle \beta, \mathbf{u} \rangle^{2ie(\sigma_*)-1} \frac{\beta}{(\kappa \rho)^{ie(\sigma_*)}} (1 + O(1/\sqrt{d})) \\ &\quad + \tilde{O}(\alpha_2^2 m^2 \sqrt{r}) + \tilde{O}(\alpha_2 m \sqrt{\frac{r}{N_2}}) + \nu. \end{aligned}$$

Considering $\mathbf{x}_i^* = \tilde{O}(\sqrt{r})$, taking the inner product of \mathbf{x}_i^* and \mathbf{h} leads to

$$\begin{aligned} \langle \mathbf{x}_i^*, \mathbf{h} \rangle &= \Theta(\alpha_2 m) \langle \beta, \mathbf{u} \rangle^{2ie(\sigma_*)-1} \frac{\langle \mathbf{x}_i^*, \beta \rangle}{(\kappa \rho)^{ie(\sigma_*)}} (1 + O(1/\sqrt{d})) \\ &\quad + \tilde{O}(\alpha_2^2 m^2 r) + \tilde{O}(\alpha_2 m r / \sqrt{N_2}) + \langle \mathbf{x}_i^*, \nu \rangle. \end{aligned}$$

Following the same argument as Lemma E.1 yields $\langle \mathbf{x}_i^*, \nu \rangle = \tilde{O}(\alpha_2 m \sqrt{r})$. Thus, by letting $\nu_* = \langle \mathbf{x}_i^*, \nu \rangle$, we obtain the assertion. □

Lemma E.5. *Set $\alpha_2 m = \tilde{\Theta}(\varepsilon/r)$, $N_2 = \tilde{\Theta}(r^2)$, $N_3 = \tilde{\Theta}(\frac{r\sqrt{r}}{\varepsilon} \log \frac{1}{\varepsilon})$ and $\eta_2 = \tilde{\Theta}(1/\sqrt{r})$ (This is exactly the same situation as Lemma E.2 and Lemma E.3). Then we have*

$$\langle \mathbf{x}_i^*, \mathbf{u}^{(j)} \rangle = \tilde{O}_d(1),$$

for all $j = 1, 2, \dots, N_3 + 1$.

Proof. When $j = 1$, \mathbf{x}_i and $\mathbf{u}^{(1)}$ are independent of each other, thus Lemma H.5 yields the desired result. Substituting the parameters into the result of Lemma E.4 yields

$$\eta_2 \langle \mathbf{x}_i^*, \mathbf{h} \rangle = \tilde{O} \left(\frac{\varepsilon}{r\sqrt{r}} (1 + O(1/\sqrt{d})) \right) + \tilde{O} \left(\frac{\varepsilon}{r\sqrt{r}} \right) + \eta_2 \nu_*,$$

where $\eta_2 \nu_* = \tilde{O}(\varepsilon/r)$. First, following the same argument to derive Eq. (9) yields

$$\left| \sum_{k=1}^j \eta_2 \nu_* \right| = \tilde{O}(\varepsilon \sqrt{j}/r),$$

for $j = 1, 2, \dots, N_3$. Since $\varepsilon \sqrt{N_3}/r = \tilde{O}_d(r^{-1/4}) = o_d(1)$, we can ignore the effect of $\eta_2 \nu_*$. Then, we can see that

$$\begin{aligned} \langle \mathbf{x}_i^*, \mathbf{u}^{(j+1)} \rangle &= \langle \mathbf{x}_i^*, \mathbf{u}^{(j)} \rangle + \eta_2 \langle \mathbf{x}_i^*, \mathbf{h} \rangle - \eta_2 \langle \mathbf{h}, \mathbf{u}^{(j)} \rangle \langle \mathbf{u}^{(j)}, \mathbf{x}_i^* \rangle - \frac{1}{2} \eta_2^2 \|\mathbf{P}_{\mathbf{u}^{(n)}} \mathbf{h}\|^2 + O((\eta_2 \|\mathbf{h}\|)^3) \\ &= \langle \mathbf{x}_i^*, \mathbf{u}^{(j)} \rangle + \langle \beta, \mathbf{u}^{(j)} \rangle^{2ie(\sigma_*)-1} \tilde{O} \left(\frac{\varepsilon}{r\sqrt{r}} \right) \left(\langle \beta, \mathbf{x}_i^* \rangle - \langle \mathbf{u}^{(j)}, \mathbf{x}_i^* \rangle \langle \beta, \mathbf{u}^{(j)} \rangle \right) \\ &\quad - \tilde{O} \left(\frac{\varepsilon}{r\sqrt{r}} \right) - \tilde{O} \left(\frac{\varepsilon^2}{r^2} \right) \end{aligned}$$

holds. Now $\langle \beta, \mathbf{x}_i^* \rangle = \tilde{O}_p(1)$ and $\langle \beta, \mathbf{u}^{(j)} \rangle \leq 1$. Therefore, if $\langle \mathbf{u}^{(j)}, \mathbf{x}_i^* \rangle = \tilde{O}_p(1)$ holds, then $\langle \mathbf{x}_i^*, \mathbf{u}^{(j+1)} \rangle = \langle \mathbf{x}_i^*, \mathbf{u}^{(j)} \rangle + \tilde{O}\left(\frac{\varepsilon}{r\sqrt{r}}\right)$. Therefore, by induction, we have

$$\langle \mathbf{x}_i^*, \mathbf{u}^{(N_3+1)} \rangle = \tilde{O}\left(\log \frac{1}{\varepsilon}\right),$$

which does not depend on d . □

This lemma allows us to use Lemma C.1. Note that $N_3 = \tilde{\Theta}\left(\frac{r\sqrt{r}}{\varepsilon} \log \frac{1}{\varepsilon}\right)$ means, by ignoring the term $\log \frac{1}{\varepsilon}$, $\varepsilon = \tilde{\Theta}\left(\frac{r\sqrt{r}}{N_3}\right)$. Now we can estimate $\langle \beta, \mathbf{x} \rangle$ using $\langle \mathbf{u}^{(N_3+1)}, \mathbf{x} \rangle$. For notational simplicity, we write $\mathbf{u}^{(N_3+1)}$ as \mathbf{u} from now on.

Lemma E.6. *Let $\mathbf{x} \sim \mathcal{N}(0, \mathbf{I}_d)$, and \mathbf{u} be a vector independent of \mathbf{x} satisfying $\|\mathbf{u}\| = 1$ and $\langle \beta, \mathbf{u} \rangle \geq 1 - \varepsilon$. Then, we have*

$$\langle \beta, \mathbf{x} \rangle = \langle \mathbf{u}, \mathbf{x} \rangle + O_p(\sqrt{2\varepsilon \log d}).$$

Proof. First, note that

$$\langle \beta, \mathbf{x} \rangle = \langle \mathbf{u}, \mathbf{x} \rangle + \langle \beta - \mathbf{u}, \mathbf{x} \rangle.$$

Since we have $\langle \beta, \mathbf{u} \rangle \geq 1 - \varepsilon$, we have that

$$\|\beta - \mathbf{u}\|^2 = \|\beta\|^2 + \|\mathbf{u}\|^2 - 2\langle \beta, \mathbf{u} \rangle \leq 2\varepsilon,$$

which yields

$$\|\beta - \mathbf{u}\| \leq \sqrt{2\varepsilon}.$$

Then, combining with Lemma H.1 yields $\langle \beta - \mathbf{u}, \mathbf{x} \rangle = O_p(\sqrt{2\varepsilon \log d})$. □

F. Training MLP layer

In this section, we show that the MLP layer can fit the polynomial σ_*^{test} . Most of the argument in this section is taken from Nishikawa et al. (2025), but we do not omit the proof for readability.

Lemma F.1. *Suppose that there exists $g(\mathbf{x})$ such that*

$$|g(\mathbf{x}) - \langle \beta, \mathbf{x} \rangle| \leq \delta.$$

Then, there exists $\pi(v, b)$ such that

$$|\mathbb{E}_{v \sim \text{Unif}\{\pm 1\}, b \sim [-\log^2 d, \log^2 d]}[\pi(v, b)\sigma(v \cdot g(\mathbf{x}) + b)] - \sigma_*(\langle \beta, \mathbf{x} \rangle)| = O(\delta(\log d)^{2\deg(\sigma_*)-2})$$

with high probability over $\mathbf{x} \sim \mathcal{N}(0, \mathbf{I}_d)$. Moreover, $\sup_{v, b} |\pi(v, b)| = \tilde{O}(1)$ holds.

Proof. Let $\sigma_*(z) = \sum_{k=0}^{\deg(\sigma_*)} s_k z^k$. Now from Lemma 9 in Damian et al. (2022), there exists $\pi'_k(v, b)$ such that $\sup_{v, b} |\pi'_k(v, b)| = O(1)$ and

$$\mathbb{E}_{v \sim \text{Unif}\{\pm 1\}, b \sim [-1, 1]}[\pi'_k(v, b)\sigma(vz + b)] = z^k$$

for any $|z| \leq 1$. If we define

$$\pi(v, b) = \sum_{k=0}^{\deg(\sigma_*)} s_k \frac{\pi'_k(v, b \log^{-2} d)}{\log^2 d} \log^{2k} d,$$

then, we have $\sup_{v,b} |\pi(v, b)| = O(\log^{2 \deg(\sigma_*) - 2} d)$. Moreover, when $|z \log^{-2} d| \leq 1$, we have

$$\begin{aligned}
 & \mathbb{E}_{v \sim \text{Unif}\{\pm 1\}, b \sim [-\log^2 d, \log^2 d]} [\pi(v, b) \sigma(vz + b)] \\
 &= \sum_{k=0}^{\deg(\sigma_*)} s_k \mathbb{E}_{v \sim \text{Unif}\{\pm 1\}, b \sim [-\log^2 d, \log^2 d]} \left[\frac{\pi'_k(v, b \log^{-2} d)}{\log^2 d} \log^{2k} d \sigma(vz + b) \right] \\
 &= \sum_{k=0}^{\deg(\sigma_*)} s_k \log^{2k-2} d \mathbb{E}_{v \sim \text{Unif}\{\pm 1\}, b \sim [-1, 1]} [\pi'_k(v, b) \sigma(\log^2 d (vz \log^{-2} d + b))] \\
 &= \sum_{k=0}^{\deg(\sigma_*)} s_k z^k = \sigma_*(z).
 \end{aligned}$$

Therefore, it holds that

$$\begin{aligned}
 & \mathbb{E}_{v \sim \text{Unif}\{\pm 1\}, b \sim [-\log^2 d, \log^2 d]} [\pi(v, b) \sigma(v \cdot g(\mathbf{x}) + b)] \\
 &= \mathbb{E}_{v \sim \text{Unif}\{\pm 1\}, b \sim [-\log^2 d, \log^2 d]} [\pi(v, b) \sigma(v \langle \beta, \mathbf{x} \rangle + v\delta + b)] \\
 &= \mathbb{E}_{v \sim \text{Unif}\{\pm 1\}, b \sim [-\log^2 d, \log^2 d]} [\pi(v, b) \sigma(v \langle \beta, \mathbf{x} \rangle + b)] + O(\delta \log^{2 \deg(\sigma_*) - 2} d) \\
 &= \sigma_*(\langle \beta, \mathbf{x} \rangle) + O(\delta \log^{2 \deg(\sigma_*) - 2} d).
 \end{aligned}$$

Here, we used the fact that $|\langle \beta, \mathbf{x} \rangle| \leq \log^2 d$ with high probability. □

Lemma F.2. *Under the condition of Lemma F.1, there exists $\mathbf{a}' \in \mathbb{R}^m$ such that*

$$\left| \sum_{j=1}^m a'_j \sigma(v_j \cdot g(\mathbf{x}) + b_j) - \sigma_*(\langle \beta, \mathbf{x} \rangle) \right| = \tilde{O}(m^{-\frac{1}{2}}) + O(\delta \log^{2 \deg(\sigma_*) - 2} d)$$

holds with high probability over $\mathbf{x} \sim (0, \mathbf{I}_d)$. Moreover, $\|\mathbf{a}'\|^2 = \tilde{O}(m^{-1/2})$ holds with high probability.

Proof. Using $\pi(v, b)$ in Lemma F.1, define $a'_j = m^{-1} \pi(v_j, b_j)$. Since $\sup_{v,b} |\pi(v, b)| = \tilde{O}(1)$, from Hoeffding's inequality, it holds that

$$\left| m^{-1} \sum_{j=1}^m \pi(v_j, b_j) \sigma(v_j \cdot g(\mathbf{x}) + b_j) - \mathbb{E}_{v,b} [\pi(v, b) \sigma(v \cdot g(\mathbf{x}) + b)] \right| = \tilde{O}(m^{-1/2}),$$

with high probability. Hence we have

$$\left| \sum_{j=1}^m a'_j \sigma(v_j \cdot g(\mathbf{x}) + b_j) - \sigma_*(\langle \beta, \mathbf{x} \rangle) \right| = \tilde{O}(m^{-\frac{1}{2}}) + O(\delta \log^{2 \deg(\sigma_*) - 2} d).$$

As for the upper bound of the norm $\|\mathbf{a}'\|^2 = m^{-1} \cdot m^{-1} \sum_{j=1}^m \pi(v_j, b_j)^2$, Hoeffding's inequality yields

$$\left| m^{-1} \sum_{j=1}^m \pi(v_j, b_j)^2 - \mathbb{E}_{v,b} [\pi(v, b)^2] \right| = \tilde{O}(m^{-1/2}).$$

Since $\sup_{v,b} |\pi(v, b)| = \tilde{O}(1)$, we can say that $\mathbb{E}_{v,b} [\pi(v, b)^2] = \tilde{O}(1)$, which completes the proof. □

Lemma F.3. *Let \mathbf{a}^* be the parameter trained via Algorithm 1. Then there exists λ_3 such that*

$$\frac{1}{N_4} \sum_{t=N_1+N_2+N_3+1}^{N_1+N_2+N_3+N_4} |y_t - f_{\text{TF}}(\mathbf{x}_t, \mathbf{u}, \mathbf{v}^*, \mathbf{a}^*, \mathbf{b}^*)| = \tau + \tilde{O}(m^{-1/2}) + O(\delta \log^{2 \deg(\sigma_*) - 2} d)$$

with high probability. Moreover, $\|\mathbf{a}^*\|^2 \leq \tilde{O}_p(m^{-1/2})$ is satisfied.

Proof. Let $M = N_1 + N_2 + N_3$ and \mathbf{a}' be the output parameter constructed in Lemma F.2: from the equivalence between ℓ_2 -regularized and norm-constrained optimization algorithms, if we carefully choose λ_3 , then we have

$$\begin{aligned} \left(\frac{1}{N_4} \sum_{t=M+1}^{M+N_4} |y_t - f_{\text{TF}}(\mathbf{x}_t, \mathbf{u}, \mathbf{v}^*, \mathbf{a}^*, \mathbf{b}^*)| \right)^2 &\leq \frac{1}{N_4} \sum_{t=M+1}^{M+N_4} (y_t - f_{\text{TF}}(\mathbf{x}_t, \mathbf{u}, \mathbf{v}^*, \mathbf{a}^*, \mathbf{b}^*))^2 \\ &\leq \frac{1}{N_4} \sum_{t=M+1}^{M+N_4} (y_t - f_{\text{TF}}(\mathbf{x}_t, \mathbf{u}, \mathbf{v}^*, \mathbf{a}', \mathbf{b}^*))^2 \\ &\leq (\tau + \tilde{O}(m^{-1/2}) + O(\delta \log^2 \text{deg}(\sigma_*)^{-2} d))^2 \end{aligned}$$

(recall that we assumed $\tau = \Theta(1)$) with high probability, which yields the first assertion. Moreover, from Lemma F.2, we can see that

$$\|\mathbf{a}^*\|^2 \leq \|\mathbf{a}'\|^2 \leq \tilde{O}_p(m^{-1/2}),$$

which completes the proof. \square

Lemma F.4. We fix \mathbf{b} and \mathbf{v} . Let $\mathcal{F}_A = \{\mathbf{a} \mapsto \sum_{i=1}^m a_i \sigma(v_j \langle \mathbf{x}, \mathbf{u} \rangle + b_j) \mid \|\mathbf{a}\| \leq A\}$ the set of transformers where the norm of the MLP parameter \mathbf{a} is upper bounded. When $\|\mathbf{b}\| \leq B$ and $v_j = \pm 1$, then it holds that

$$\text{Rad}_N(\mathcal{F}_A) = \tilde{O}\left(\frac{A(B + \sqrt{m})}{\sqrt{N_4}}\right).$$

Proof. Note that $\mathbb{E}[g(\mathbf{x})^2] = \mathbb{E}[\langle \mathbf{u}, \mathbf{x} \rangle^2] = O(\log d)$, considering $\|\mathbf{u}\| = 1$. Then, following the same argument as Lemma 25 in Nishikawa et al. (2025) yields the assertion. \square

G. Proof of the Theorem 1.1

Now, we are ready to give the proof of Theorem 1.1.

Proof. First note that

$$\begin{aligned} \mathcal{R}_{f_{\text{TF}}}(\mathbf{u}, \mathbf{v}^*, \mathbf{a}^*, \mathbf{b}^*) - \tau &= \frac{1}{N_4} \sum_{i=N_1+N_2+N_3+1}^{N_1+N_2+N_3+N_4} |y_i - f_{\text{TF}}(\mathbf{x}_i, \mathbf{u}, \mathbf{v}^*, \mathbf{a}^*, \mathbf{b}^*)| - \tau \\ &\quad + \mathcal{R}_{f_{\text{TF}}}(\mathbf{u}, \mathbf{v}^*, \mathbf{a}^*, \mathbf{b}^*) - \frac{1}{N_4} \sum_{i=N_1+N_2+N_3+1}^{N_1+N_2+N_3+N_4} |y_i - f_{\text{TF}}(\mathbf{x}_i, \mathbf{u}, \mathbf{v}^*, \mathbf{a}^*, \mathbf{b}^*)|. \end{aligned}$$

From Lemma F.3, the first two terms $\frac{1}{N_4} \sum_{i=N_1+N_2+N_3+1}^{N_1+N_2+N_3+N_4} |y_i - f_{\text{TF}}(\mathbf{x}_i, \mathbf{u}, \mathbf{v}^*, \mathbf{a}^*, \mathbf{b}^*)| - \tau$ are bounded by $\tilde{O}(m^{-1/2}) + O(\delta \log^2 \text{deg}(\sigma_*)^{-2} d)$. Moreover, from Lemma F.2 and the definition of \mathbf{b}^* , we have $\|\mathbf{a}^*\| = \tilde{O}(m^{-1/2})$ and $\|\mathbf{b}^*\| = \tilde{O}(\sqrt{m})$. Therefore, from Lemma F.4, we have

$$\text{Rad}_N(\mathcal{F}_A) = \tilde{O}(N_4^{-1/2}).$$

Using the standard technique yields (see Appendix D.3 in Oko et al. (2024))

$$|\mathcal{R}_{f_{\text{TF}}}(\mathbf{u}, \mathbf{v}^*, \mathbf{a}^*, \mathbf{b}^*) - \tau| = \tilde{O}(N_4^{-1/2}) + \tilde{O}(m^{-1/2}) + O(\delta \log^2 \text{deg}(\sigma_*)^{-2} d),$$

with probability at least 0.995. Note that all the desired events occur with high probability, except for this event. Therefore, when d is large enough, all the events occur with probability at least 0.99.

Finally, we rewrite the term $O(\delta \log^2 \text{deg}(\sigma_*)^{-2} d)$. From Lemma E.6, $\delta = O(\sqrt{2\varepsilon \log d})$ holds. Also, $N_3 = \tilde{\Theta}(\frac{r\sqrt{r}}{\varepsilon} \log \frac{1}{\varepsilon})$, which means, when we ignore the term $\log \frac{1}{\varepsilon}$, $\varepsilon = \tilde{\Theta}(\frac{r\sqrt{r}}{N_3})$. Therefore

$$O(\delta \log^2 \text{deg}(\sigma_*)^{-2} d) = \tilde{O}\left(\sqrt{\frac{r\sqrt{r}}{N_3}}\right)$$

is satisfied. This completes the proof. \square

H. Additional Lemmas

Lemma H.1. Suppose $\mathbf{x} \sim \mathcal{N}(0, \mathbf{I}_d)$ and \mathbf{y} is a vector satisfying $\|\mathbf{y}\| = C$ independent of \mathbf{x} . Then

$$\langle \mathbf{x}, \mathbf{y} \rangle = O(C\sqrt{\log d})$$

holds with high probability.

Lemma H.2. Let z_1, \dots, z_n be i.i.d. random variables which satisfy $\|z_i\| \leq C$ with high probability and $\mathbb{E}[z_i^2] = O(d^\alpha)$, where α is a constant independent of d . When $n = \text{poly}(d)$,

$$\frac{1}{n} \sum_{i=1}^n z_i - \mathbb{E}[z_i] = O\left(C\sqrt{\frac{1}{n}}\right)$$

holds with high probability.

Proof. Let $z'_i = z_i \mathbf{1}_{|z_i| \leq C}$. Applying the uniform bound argument, we may consider that $z_i = z'_i$ for all $i = 1, \dots, n$ with high probability because our assumption $n = \text{poly}(d)$ yields

$$P(\max_i |z_i| \leq C) \geq 1 - O(nd^{-C_*}) \geq 1 - O(d^{-C'_*}),$$

where C'_* is a constant determined appropriately. Then, using Hoeffding's inequality yields

$$\frac{1}{n} \sum_{i=1}^n z_i - \mathbb{E}[z'_i] = O\left(C\sqrt{\frac{1}{n}}\right).$$

We complete the proof by showing that $|\mathbb{E}[z_i] - \mathbb{E}[z'_i]|$ is sufficiently small. This can be shown by

$$\begin{aligned} \mathbb{E}[z_i] - \mathbb{E}[z'_i] &= \mathbb{E}[z_i \mathbf{1}_{|z_i| > C_*}] \\ &\leq \mathbb{E}[\mathbf{1}_{|z_i| > C_*}]^{1/2} \mathbb{E}[z_i^2]^{1/2} \\ &\leq O(d^{\alpha - C_*}), \end{aligned}$$

where C_* can be taken sufficiently large from the definition of high probability event. Since we assumed that $n = \text{poly}(d)$, this term is smaller than the main term, which completes the proof. \square

Lemma H.3 ((Damian et al., 2023), Property 1). Let $\alpha, \beta \in \mathbb{S}^{d-1}$, then

$$\mathbb{E}_{\mathbf{x} \sim \mathcal{N}(0, \mathbf{I}_d)} [\text{He}_i(\langle \alpha, \mathbf{x} \rangle) \text{He}_i(\langle \beta, \mathbf{x} \rangle)] = \mathbf{1}_{i=j} i! \langle \alpha, \beta \rangle^i.$$

H.1. Pretrained matrix

Let Γ^* be a matrix obtained after pretraining. Then, from Nishikawa et al. (2025), Γ^* can be written as

$$\Gamma^* = \frac{r \mathbb{E}_\beta [\beta \beta^\top] + \mathbf{N}}{\kappa \sqrt{r}}$$

for some matrix \mathbf{N} satisfying $\|\mathbf{N}\|_F = O(1/\sqrt{d})$ and a number $\kappa = \Theta(\log^{C_\kappa} d)$. Also, from Nishikawa et al. (2025) and the assumption on the support of β ,

$$\mathbf{U}\beta \sim \text{Unif}\{(\alpha_1, \alpha_2, \dots, \alpha_r, 0, \dots, 0) \mid \alpha_1^2 + \dots + \alpha_r^2 = 1\}.$$

holds for some orthogonal matrix \mathbf{U} . Then, using $\mathbf{D} = \text{diag}(\underbrace{1, \dots, 1}_r, \underbrace{0, \dots, 0}_{d-r})$, we have that $r \mathbb{E}_\beta [\beta \beta^\top] = \mathbf{U}^\top \mathbf{D} \mathbf{U}$.

Lemma H.4. Let $\mathbf{x} \sim \mathcal{N}(0, \mathbf{I}_d)$, then

$$\|\sqrt{r} \kappa \Gamma^* \mathbf{x}\| = \tilde{O}(\sqrt{r})$$

holds with high probability.

Proof. By the argument above, we can write that

$$\sqrt{r}\kappa\Gamma^*\mathbf{x}=(U^\top DU+N)\mathbf{x}.$$

From rotational invariance, when we define \mathbf{y} as $\mathbf{y}=\mathbf{U}\mathbf{x}$, $\mathbf{y}\sim\mathcal{N}(0,\mathbf{I}_d)$ is satisfied. From the definition of \mathbf{D} , the first r components of $\mathbf{D}\mathbf{y}$ follow standard normal distribution i.i.d., and the other $(n-r)$ components are equal to zero. Since applying U^\top to a vector does not change the norm of the vector, we obtain

$$U^\top DU\mathbf{x}=U^\top D\mathbf{y}=\tilde{O}(\sqrt{r}),$$

with high probability. Finally, since $\|\mathbf{N}\|_F=O(1/\sqrt{d})$, $\mathbf{N}\mathbf{x}=\tilde{O}(1)$ holds. Hence we can ignore the term $\mathbf{N}\mathbf{x}$. \square

Lemma H.5. *Let $\mathbf{x}\sim\mathcal{N}(0,\mathbf{I}_d)$, and \mathbf{u} be a vector independent of \mathbf{x} satisfying $\|\mathbf{u}\|=1$. then*

$$\langle\sqrt{r}\kappa\Gamma^*\mathbf{x},\mathbf{u}\rangle=O(\sqrt{\log d})$$

holds with high probability.

Proof. As in the previous lemma, we know that

$$\sqrt{r}\kappa\Gamma^*\mathbf{x}=(U^\top DU+N)\mathbf{x}$$

holds. Again, from rotational invariance, when we define \mathbf{y} as $\mathbf{y}=\mathbf{U}\mathbf{x}$, $\mathbf{y}\sim\mathcal{N}(0,\mathbf{I}_d)$ is satisfied. From the definition of \mathbf{D} , the first r components of $\mathbf{D}\mathbf{y}$ follow standard normal distribution i.i.d., and the other $(n-r)$ components are equal to zero. Also, when we define $\mathbf{u}'=\mathbf{U}\mathbf{u}$, we have $\|\mathbf{u}'\|=1$, which means $\sqrt{u_1'^2+\dots+u_r'^2}\leq 1$. Therefore, from Corollary 30 in Nishikawa et al. (2025), we have

$$\langle U^\top DU\mathbf{x},\mathbf{u}\rangle=\langle D\mathbf{y},\mathbf{u}'\rangle=O_p(\sqrt{\log d}).$$

As for $\mathbf{N}\mathbf{x}$, again from Corollary 30 in Nishikawa et al. (2025), we have

$$\langle\mathbf{N}\mathbf{x},\mathbf{u}\rangle=O_p\left(\sqrt{\frac{\log d}{d}}\right).$$

This is smaller than the main term. \square

Lemma H.6. *Let $\mathbf{x}_1\dots\mathbf{x}_n\sim\mathcal{N}(0,\mathbf{I}_d)$, and z_1,\dots,z_n are i.i.d. random variables which satisfy $|z_i|\leq C_z$ with high probability. When $n=\text{poly}(d)$, it holds that*

$$\left\|\frac{1}{n}\sum_{i=1}^n(z_i\sqrt{r}\kappa\Gamma^*\mathbf{x}_i)-\mathbb{E}[z_1\sqrt{r}\kappa\Gamma^*\mathbf{x}_1]\right\|=\tilde{O}\left(C_z\sqrt{\frac{r}{n}}\right),$$

with high probability.

Proof. We use the same proof strategy as Lemma 31 in Nishikawa et al. (2025). Let $z'_i=z_i\mathbf{1}_{|z_i|\leq C_z}$. First, we can confirm that

$$\begin{aligned}\mathbb{E}[z_1\sqrt{r}\kappa\Gamma^*\mathbf{x}_1]-\mathbb{E}[z'_1\sqrt{r}\kappa\Gamma^*\mathbf{x}_1]&=\mathbb{E}[\mathbf{1}_{|z_1|>C_z}\sqrt{r}\kappa\Gamma^*\mathbf{x}_1] \\ &\leq\mathbb{E}[\mathbf{1}_{|z_1|>C_z}^2]^{1/2}\mathbb{E}[\|\sqrt{r}\kappa\Gamma^*\mathbf{x}_1\|^2]^{1/2} \\ &\leq O(d^{-C}).\end{aligned}$$

Where C can be taken sufficiently large from the definition of high probability event. Because $n=\text{poly}(d)$, by redefining C if necessary, we can make this term smaller than $\tilde{O}(C_z\sqrt{\frac{r}{n}})$. As $\frac{1}{n}\sum_{i=1}^n(z_i\sqrt{r}\kappa\Gamma^*\mathbf{x}_i)=\frac{1}{n}\sum_{i=1}^n(z'_i\sqrt{r}\kappa\Gamma^*\mathbf{x}_i)$ with high probability, we continue to evaluate $\frac{1}{n}\sum_{i=1}^n(z'_i\sqrt{r}\kappa\Gamma^*\mathbf{x}_i)-\mathbb{E}[z'_1\sqrt{r}\kappa\Gamma^*\mathbf{x}_1]$. Let $\mathbf{y}_i=\mathbf{U}\mathbf{x}_i$. Then $\mathbf{y}_i\sim\mathcal{N}(0,\mathbf{I}_d)$

holds. $z'_i \mathbf{D} \mathbf{y}_i$ is a sub-Gaussian vector, and $(\mathbf{D} \mathbf{y}_i)_k = 0$ when $k > r$ from the definition of \mathbf{D} . Then, applying a standard concentration bound for a sub-Gaussian vector to the r -dimensional vector $(\mathbf{D} \mathbf{y}_i)_{1:r}$ yields

$$\frac{1}{n} \sum_{i=1}^n z'_i \mathbf{D} \mathbf{y}_i - \mathbb{E}[z'_1 \mathbf{D} \mathbf{y}_1] = \tilde{O} \left(C_z \sqrt{\frac{r}{n}} \right).$$

As multiplying the orthogonal matrix U^\top does not change the norm of the vector, we have

$$\frac{1}{n} \sum_{i=1}^n z'_i U^\top \mathbf{D} U \mathbf{x}_i - \mathbb{E}[z'_1 U^\top \mathbf{D} U \mathbf{x}_1] = \tilde{O} \left(C_z \sqrt{\frac{r}{n}} \right).$$

Again from the standard concentration bound for a sub-Gaussian vector, we have

$$\frac{1}{n} \sum_{i=1}^n z'_i \mathbf{x}_i - \mathbb{E}[z'_1 \mathbf{x}_1] = \tilde{O} \left(C_z \sqrt{\frac{d}{n}} \right),$$

with high probability. Since $\|\mathbf{N}\|_F = O(1/\sqrt{d})$, we have

$$\frac{1}{n} \sum_{i=1}^n z'_i \mathbf{N} \mathbf{z}_i - \mathbb{E}[z'_1 \mathbf{N} \mathbf{x}_1] = \tilde{O} \left(C_z \sqrt{\frac{1}{n}} \right).$$

In summary, we arrive at

$$\begin{aligned} & \frac{1}{n} \sum_{i=1}^n (z_i \sqrt{r} \kappa \Gamma^* \mathbf{x}_i) - \mathbb{E}[z_1 \sqrt{r} \kappa \Gamma^* \mathbf{x}_1] \\ &= \frac{1}{n} \sum_{i=1}^n (z_i (U^\top \mathbf{D} U + \mathbf{N}) \mathbf{x}_i) - \mathbb{E}[z_1 (U^\top \mathbf{D} U + \mathbf{N}) \mathbf{x}_1] = \tilde{O} \left(C_z \sqrt{\frac{r}{n}} \right), \end{aligned}$$

with high probability, which completes the proof. \square

Lemma H.7. *We have that*

$$\sqrt{r} \kappa \Gamma^* \beta = \beta + O(1/\sqrt{d}).$$

Proof. First note that

$$\sqrt{r} \kappa \Gamma^* \beta = (U^\top \mathbf{D} U + \mathbf{N}) \beta.$$

From the definition of U , we have $U \beta = (\alpha_1, \alpha_2, \dots, \alpha_r, 0, \dots, 0)^\top$ for some $\alpha_1, \alpha_2, \dots, \alpha_r \in \mathbb{R}$. Therefore, we obtain that

$$U^\top \mathbf{D} U \beta = U^\top U \beta = \beta.$$

Finally, by noticing $\|\mathbf{N}\|_F = O(1/\sqrt{d})$ and $\|\beta\| = 1$, we can see that $\mathbf{N} \beta = O(1/\sqrt{d})$ holds. \square

Lemma H.8. *We have that*

$$\sqrt{r} \kappa \Gamma^* (\sqrt{r} \kappa \Gamma^* \beta) = \beta + O(1/\sqrt{d}).$$

Proof. From lemma H.7, we have $\sqrt{r} \kappa \Gamma^* \beta = \beta + \mathbf{d}$ where $\mathbf{d} = O(1/\sqrt{d})$. Therefore, it holds that

$$\sqrt{r} \kappa \Gamma^* (\sqrt{r} \kappa \Gamma^* \beta) = \sqrt{r} \kappa \Gamma^* (\beta + \mathbf{d}).$$

Again from Lemma H.7, we see that $\sqrt{r} \kappa \Gamma^* \beta = \beta + O(1/\sqrt{d})$. Also we have $\sqrt{r} \kappa \Gamma^* \mathbf{d} = U^\top \mathbf{D} U \mathbf{d} + \mathbf{N} \mathbf{d}$, and since $\|U^\top \mathbf{D} U\|_2 = 1$ from the definition of U and \mathbf{D} , we have $U^\top \mathbf{D} U \mathbf{d} = O(1/\sqrt{d})$. Finally, since $\|\mathbf{N}\|_F = O(1/\sqrt{d})$, we have $\mathbf{N} \mathbf{d} = O(1/d)$. This indicates that $\sqrt{r} \kappa \Gamma^* \mathbf{d} = O(1/\sqrt{d})$. \square

I. Experimental details

The GPT-2 model architecture we used in Section 4 originates from Garg et al. (2023). Given the $(N + 1)$ -length prompt $\{(\mathbf{x}_i, y_i)\}_{i=1}^{N+1}$, we first construct the embedding as

$$\mathbf{E} = [\mathbf{x}_1, \tilde{\mathbf{y}}_1, \dots, \mathbf{x}_{N+1}, \tilde{\mathbf{y}}_{N+1}] \in \mathbb{R}^{d \times (2N+2)},$$

where $\tilde{\mathbf{y}}_i = [y_i, 0, \dots, 0]^\top$. Next, the read-in layer transforms this embedding into $\tilde{\mathbf{E}} \in \mathbb{R}^{D \times (2N+2)}$, where $D = 128$. This mapped embedding $\tilde{\mathbf{E}}$ goes through a 2-layer GPT-2 backbone with 4 attention heads, following the configuration by Garg et al. (2023). Finally, the output of GPT-2 backbone is transformed by the read-out layer into the vector $[z_1, z_2, \dots, z_{2N+1}, z_{2N+2}]$. Here, z_{2i-1} is the prediction of y_i given the context $(\mathbf{x}_1, y_1, \dots, \mathbf{x}_{i-1}, y_{i-1}, \mathbf{x}_i)$. We used Adam optimizer (Kingma & Ba, 2017) with a learning rate of 0.0001. To reduce the pretraining cost, we adopted the curriculum learning strategy, which is also used in Garg et al. (2023). The training started with the dimension $d = 4$, and the dimension was increased by two until it reached the target dimension.

For the model with TTT, we introduced low-rank adaptation (LoRA) to the attention projection layers (c_attn and c_proj) and the feedforward layer (c_fc) of the base model. The rank of LoRA was set to 4, and the parameters LoRA_alpha and LoRA_dropout were set to 8 and 0.1, respectively. The LoRA parameters were updated 300 times via SGD for each query. The inference-time learning rate was 0.1 in the experiment in Figure 1 and Figure 2. To prevent information leakage when evaluating the prediction of y_i , the model used only the preceding data $(\mathbf{x}_1, y_1, \dots, \mathbf{x}_{i-1}, y_{i-1}, \mathbf{x}_i)$ to update the weight. The LoRA weights were reset before proceeding to the prediction of the next target, y_{i+1} . We observed numerical instability (gradient explosion) in a negligible fraction of trials; these instances were excluded from the final results to ensure metric stability.

The test loss was averaged over 256 runs, with each run containing 256 independent queries.